Science of the Total Environment 924 (2024) 171441

Contents lists available at ScienceDirect

Science of the Total Environment

journal homepage: www.elsevier.com/locate/scitotenv

# Impact of single and combined local air pollution mitigation measures in an urban environment

J.L. Santiago [a,*], E. Rivas [a,b], B. Sanchez [a], R. Buccolieri [c,d], M.G. Vivanco [a], A. Martilli [a], F. Martín [a]

[a] Atmospheric Modelling Unit, Environmental Department, CIEMAT, Av. Complutense 40, 28040 Madrid, Spain
[b] Vicerrectorado de Investigación, Innovación y Doctorado, Universidad Politécnica de Madrid (UPM), Madrid, Spain
[c] Department of Environmental and Biological Sciences and technologies, Laboratory of Micrometeorology, University of Salento, S.P. 6 Lecce-Monteroni, 73100 Lecce, Italy
[d] Institute of Atmospheric Sciences and Climate (ISAC), National Research Council (CNR), S.P. Lecce-Monteroni km 1,2, 73100 Lecce, Italy

## HIGHLIGHTS

- Local air pollution mitigation measures are evaluated by CFD modelling.
- Not all Green Infrastructure (GI) are effective due to reduction of street ventilation
- Low Emission Zones (LEZ) is the most effective single measure studied.
- For some scenarios, the combination GI + LEZ is more effective than an individual LEZ
- Negative effects of GI can turn into positive if traffic emissions are reduced.

## GRAPHICAL ABSTRACT

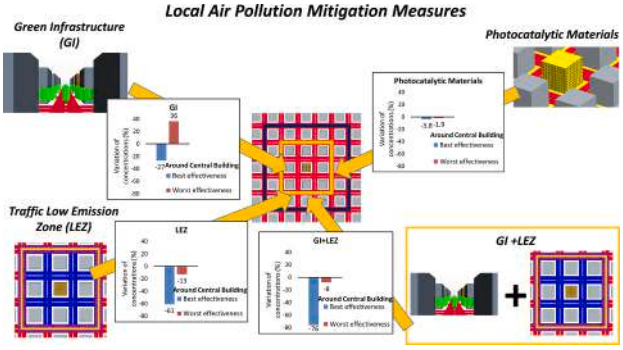


## ARTICLE INFO

Editor: Anastasia Paschalidou

*Keywords:*
Computational fluid dynamics (CFD) modelling
Green infrastructure (GI)
Low emission zones (LEZ)
Photocatalytic materials
Traffic-related air pollution
Urban air quality

## ABSTRACT

Urban air pollution is one of the most important environmental problems for human health and several strategies have been developed for its mitigation. The objective of this study is to assess the impact of single and combined mitigation measures on concentrations of air pollutants emitted by traffic at pedestrian level in the same urban environment. The effectiveness of different scenarios of green infrastructure (GI), the implementation of photocatalytic materials and traffic low emission zones (LEZ) are investigated, as well as several combinations of LEZ and GI. A wide set of scenarios is simulated through Computational Fluid Dynamics (CFD) modelling for two different wind directions (perpendicular (0°) and 45° wind directions). Wind flow for the BASE scenario without any measure implemented was previously evaluated using wind-tunnel measurements. Air pollutant concentrations for this scenario are compared with the results obtained from the different mitigation scenarios. Reduction of traffic emissions through LEZ is found to be the most effective single measure to improve local air quality. However, GI enhances the effects of LEZ, which makes the combination of LEZ + GI a very effective measure. The effectiveness of this combination depends on the GI layout, the intensity of emission reduction in the LEZ and the traffic diversion in streets surrounding the LEZ. These findings, in line with previous literature,

* Corresponding author.
*E-mail address:* jl.santiago@ciemat.es (J.L. Santiago).

https://doi.org/10.1016/j.scitotenv.2024.171441
Received 17 October 2023; Received in revised form 22 February 2024; Accepted 1 March 2024
Available online 4 March 2024

suggest that the implementation of GI may increase air pollutant concentrations at pedestrian level for some cases. However, this study highlights that this negative effect on air quality can turn into positive when used in combination with reductions of local traffic emissions.

## 1. Introduction

High levels of air pollutants such as nitrogen oxides (NOx) and particulate matter (e.g., PM2.5, PM10) are usually found in urban environments. Due to the fact that most of the people live in cities, a great part of population is exposed to atmospheric pollutant concentrations above the air quality standards (EEA, 2020). Hence, urban air pollution is one of the most important problems for human health (WHO, 2018). Different local measures for improving urban air quality are being implemented in most cities. Among these measures, the most common are:

- Emission reduction measures such as Low Emission Zones (LEZ) (Boogaard et al., 2012; Holman et al., 2015; Huang et al., 2021; Santiago et al., 2022a), where traffic is restricted or banned in some urban areas decreasing local emissions of air pollutants. The restrictions of LEZs established in cities affects different vehicle types, and, consequently, the range of emission reductions is wide depending on LEZ restrictions. Information regarding LEZ established in European cities can be found in the website portal (https://urbanaccessregulations.eu) developed with the support of the European Commission. In this study, a wide range of LEZ scenarios is investigated;
- photocatalytic materials, a technology for air purification that incorporates compounds such as titanium dioxide, which are activated in the presence of solar radiation and allow the elimination of air pollutants such as NOx (Fernández-Pampillón et al., 2021; Sanchez et al., 2021). Therefore, these materials mainly affect NOx concentrations;
- green Infrastructure (GI). GI composed by trees and hedgerows is one of the most used passive control systems for air pollution in street canyons, although optimum GI design is currently unclear (Gallagher et al., 2015; Li et al., 2021; Tomson et al., 2021; Buccolieri et al., 2022).

The interactions between atmosphere and buildings induce complex wind flow and reduced ventilation in the streets producing high levels and strong gradients of air pollutant concentrations released from traffic (Borge et al., 2016; Santiago et al., 2017a). Hence, studies (experimental campaigns or numerical simulations) at high spatial resolution are necessary to determine the distribution of air pollutant concentrations in urban environments. Therefore, air quality, population exposure to atmospheric pollution and the impact of mitigation or abatement measures are difficult to assess in the cities (Vardoulakis et al., 2011; Santiago et al., 2013; Di Sabatino et al., 2013; Gromke and Blocken, 2015; Kracht et al., 2018; Santiago et al., 2020; Santiago et al., 2021; Santiago et al., 2022b; Santiago et al., 2022c). Regarding LEZs, Holman et al. (2015) reviewed their efficacy to improve urban air quality in several European cities. Some evidence of the reduction of long-term average PM10 and $NO_2$ was found, although separating the direct effects of a LEZ from the effects of other policy measures, the economy, and the normal renewal of the vehicle fleet was not easy. Therefore, theoretical studies considering different scenarios of LEZ are useful to understand their effectiveness. Concerning photocatalytic materials, Fernández-Pampillón et al. (2021) and Sanchez et al. (2021) showed that robust experimental campaigns and numerical simulations at high spatial resolution are needed to demonstrate the efficiency of photocatalytic materials at real scale. Further, assessing the impacts of GI is more complex than other measures due to the different effects of vegetation on air quality. These effects can be summarized as follows (Abhijith et al., 2017; Buccolieri et al., 2018a):

- aerodynamic effects are due to the variation of wind flow induced by the presence of vegetation. Vegetation is a porous obstacle that modifies the wind flow. These variations of the wind flow (e.g. changing of recirculation areas, reduction of the wind speed, etc.…) change the air pollutant dispersion regardless pollutants are gaseous or particulate. The simplest parameterization of the aerodynamic effects of vegetation is through roughness. However, at microscale, the vegetation should be explicitly solved as a porous obstacle using sink/source terms in the momentum and turbulence equations (see Section 2.2);
- deposition on leaves and absorption through stomata. A fraction of atmospheric pollutants is removed from the air via deposition on leaves and absorption through stomata. Vegetation increases both the surface roughness (slowing air flow and enhancing deposition and absorption pollutant removal processes) and increases the area of surface that air pollutants come into contact with (acting as biological filters, enhanced by surface properties). Vegetation absorbs gaseous pollutants such as NOx, mainly by uptake via leaf stomata or surface, and accumulate airborne particulates by interception, impaction or sedimentation more effectively than other urban surfaces (Escobedo and Nowak, 2009; Janhäll, 2015; Buccolieri et al., 2018a, 2018b). Hence, absorption and deposition effects are different for gaseous and particulate pollutants. Deposition effects are modelled in CFD simulations through a deposition velocity which depends on the type of pollutant and plant species. For particulate pollutants, deposition is higher than for gaseous ones, but many discrepancies between deposition velocity values are found in the literature (Buccolieri et al., 2018b);
- biogenic emissions. Trees emit biogenic volatile organic compounds (VOCs) as a reaction to stress in their environment. In addition, pollen is also released by trees depending on several environmental factors, including local meteorological conditions.

In the streets, estimating the net effect of GI on air quality is more difficult. Deposition effects always improve air quality, while aerodynamic effects can be positive or negative. Most studies have found that the contribution of aerodynamic effects on air pollutant concentrations in the streets is higher than the deposition contribution (Vos et al., 2013; Vranckx et al., 2015; Jeanjean et al., 2017a; Santiago et al., 2017b; Santiago et al., 2017c; Santiago et al., 2019a). This fact means that the impact of modification of wind flow due to the presence of trees on air quality in the streets is more important than the air pollutant concentration removal via deposition on leaves. However, both effects can have major impacts depending on the conditions (meteorological conditions, urban morphology and vegetation characteristics) (Jeanjean et al., 2017a; Santiago et al., 2017c; Xue and Li, 2017; Buccolieri et al., 2018b; Santiago et al., 2022d). In the streets, trees act as obstacles to the wind and usually diminish the turbulent exchange of mass and momentum between the air above the canopy and within the street depending on shape and configuration (Abhijith et al., 2017). Therefore, in general, aerodynamic effects of street trees tend to reduce the potential ventilation of the street, and, consequently, airborne concentrations of particulate and gaseous pollutants increase at pedestrian levels (Vos et al., 2013; Vranckx et al., 2015; Gromke and Blocken, 2015; Abhijith et al., 2017; Jeanjean et al., 2017a; Kumar et al., 2019; Tomson et al., 2021; Santiago et al., 2022d). However, a few studies (Amorim et al., 2013; Abhijith et al., 2017; Jeanjean et al., 2017a; Rafael et al., 2018; Santiago et al., 2022d) have found improvements in air quality

under certain conditions. Jeanjean et al. (2017a) found decreases of NOx and PM2.5 concentrations for wind parallel to the study street. Similarly, Amorim et al. (2013) found a reduction in air pollutant concentration under parallel winds. This issue has not yet been well studied and few investigations have analyzed the relative contribution of each effect towards the net impact of GI (Buccolieri et al., 2018a, 2018b). The net impact of GI may increase or decrease air pollutant concentrations at the pedestrian level depending on several factors (e.g., green infrastructure layout, urban morphology, typical meteorological conditions, vegetation characteristics, etc.) (Tomson et al., 2021). However, the complexity of urban meteorology at street level and the limited available studies make it difficult to provide holistic recommendations (Tomson et al., 2021). A general recommendation for improving urban air quality is to implement the right GI configurations in the right streets (Buccolieri et al., 2018a, 2018b). However, it is difficult to determine the appropriate GI in each case depending on several factors such as type of streets, building morphology, type of trees, predominant meteorology, and location of pollutant sources.

On the other hand, GI provides additional environmental benefits such as micro-climate regulation, noise reduction or rainwater drainage (Salmond et al., 2016; Livesley et al., 2016; Santamouris et al., 2018), and other benefits such as aesthetic, recreational, psycho-logical or improving perceived mental health (Roy et al., 2012; Haaland and van Den Bosch, 2015; Van den Berg et al., 2015). However, several disservices are also associated with urban vegetation such as emission of biogenic volatile compounds and pollen or the cost of maintenance, irrigation, etc. (Roy et al., 2012). GI design should be addressed to obtain a trade-off solution between different ecosystem services and disservices provided (Santiago et al., 2022d). Therefore, to take advantage of all of these benefits, the impact of GI scenarios that could potentially provide adverse effects on air quality should be identified to be modified or discarded.

In this context, the first research question is to determine what is the effectiveness of each single measure (LEZ, GI and photocatalytic materials) under the same conditions. In addition, due to the numerous ecosystem services provided by urban vegetation, the second research question that arise is to estimate whether the impact of GI scenarios can be improved by combining GI with other air pollution mitigation measures. Recent results from Santiago et al. (2022d) indicate that street trees can act as a barrier for the air pollutants emitted outside the zone with GI. This fact suggests that GI implementation in combination with traffic-emission reductions in the same area may enhance the benefits on air quality.

Therefore, the main objective of this paper is to assess the impact of different local air pollution mitigation measures on traffic-related air pollutant concentrations at pedestrian level in the same urban environment. Several individual mitigation measures such as LEZ, GI and photocatalytic materials, and also, multiple combinations of GI configurations with LEZs are investigated. The starting hypotheses are:

- Concentrations of air pollutants emitted by traffic such as NOx, PM10, PM2.5 or Black Carbon can be estimated at pedestrian level.
- The effects of each single measure on these concentrations are different and spatially heterogeneous at pedestrian level.
- The impacts of different GI configurations would be positive or negative, but negative effects would be improved combining GI with LEZ.

For this purpose, several novel aspects are addressed in this study:

- a wide set of scenarios, including several configurations for each measure, is investigated by means of computational fluid dynamic (CFD) simulations. On the other hand, few studies (Jeanjean et al., 2017b) evaluated the impact of different measures for the same urban configuration. In this paper, all the scenarios are assessed for the same urban environment. This approach allows the evaluation of the effectiveness of each measure by comparing it with a reference case without additional measures (BASE case);
- not only the area with the implemented measures is simulated, but also the surrounding streets, allowing to evaluate the effects of measures not only on air pollutants emitted in the study area with the implemented measures but also on air pollutants emitted outside. The present study is focused on air pollutants emitted by traffic. NOx, as the sum of NO and $NO_2$, emitted by traffic is investigated in this study. NO and NO2 are highly reactive and dependent on $O_3$ concentrations in the streets. However, $NO+NO_2$ (NOx) can be considered as non-reactive pollutant at microscale (Sanchez et al., 2016). Regarding particulate matter (PM), PM directly emitted by traffic is investigated in the present study. Secondary production of PM due to chemical reactions is not considered. However, these assumptions are reasonable for the simulation domain considered as shown in previous studies where NOx, PM10, PM2.5 or Black Carbon were successfully considered as non-reactive in CFD simulations (Sanchez et al., 2017; Santiago et al., 2020; Jeanjean et al., 2017a; Santiago et al., 2019b);
- the effects of combining GI configurations with LEZs are also investigated.

In Section 2, the study urban area, CFD model and the air pollution mitigation strategies simulated are described. The results on the impact of LEZ, photocatalytic materials and GI are shown in Sections 3.1, 3.2 and 3.3, respectively. The effects of the combination of several GI configurations with LEZs are studied in Section 3.4. The discussion and conclusions are finally presented in Section 4.

## 2. Materials and methods

### 2.1. Description of urban geometry and local air pollution mitigation measures

An idealized urban-like environment composed by an array of 7 × 7 buildings is used for this study (Fig. 1). This domain covers not only the area where the measures are implemented but also the surrounding streets. Building height is 35 m and the aspect ratio defined as the ratio between the building height and the width of the streets is 1. This is a typical value of street canyons in real cities (e.g. Soulhac and Salizzoni, 2010; Chatzidimitriou and Yannas, 2017; Murena and Toscano, 2023).

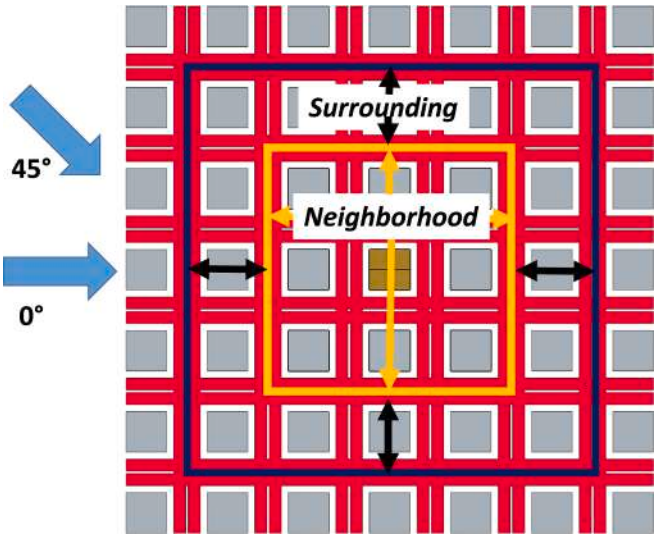


**Fig. 1.** Array of buildings within the simulation domain. The orange rectangle is the neighborhood area where measures are implemented (study area). Red indicates the emission areas. Arrows indicate the two wind directions simulated.

The packing density, defined as the ratio of the plan-built area occupied by buildings to the total study area, is 0.25. This value is within the range of planar area indexes that typically occur in urban areas (Grimmond and Oke, 1999). This urban geometry has been used in previous studies (Santiago et al., 2022c; Santiago et al., 2022d).

The investigated local air pollution mitigation measures are implemented in the central area of the study zone (Neighborhood from now on, see the orange square in Fig. 1). This allows investigating the effects of the different measures on concentration of air pollutants emitted in and outside Neighborhood (where measures are implemented). In addition, these effects are analyzed not only in Neighborhood but also in the surrounding streets (see the black square in Fig. 1). In the present paper, air pollutants emitted by traffic such as NOx ($NO+NO_2$), PM10, PM2.5 and Black Carbon are investigated. These pollutants are considered as non-reactive, assumption that is reasonable for the simulation domain considered as shown in previous studies (Sanchez et al., 2017; Santiago et al., 2020; Jeanjean et al., 2017a; Santiago et al., 2019b). As mentioned above, the mitigation measures investigated are: the use of photocatalytic materials, the implementation of LEZ with different characteristics, GI planting and the combination of GI planting with LEZ.

- *Photocatalytic materials*. These materials under solar radiation reduce air concentration of NOx. They mainly remove NO from air, however, for simplicity, in this study their effects are modelled through a constant deposition velocity of NOx to quantify the pollutant flux that is removed from air. A value of 0.005 m $s^{-1}$ is selected (Fernández-Pampillón et al., 2021; Sanchez et al., 2021; Palacios et al., 2015). Two scenarios are simulated: in *Photocat_G* scenario, the implementation is only on the ground in the sidewalks of Neighborhood. In *Photocat_GWR* scenario, photocatalytic materials are implemented on the ground in the sidewalks of Neighborhood and on walls and roof of the central building (yellow in Fig. 2). Note that CFD simulations with a similar set-up to model photocatalytic materials (Sanchez et al., 2021; Pulvirenti et al., 2020) were able to reproduce field experimental observations).

- *Low emission zones* (*LEZ*). Traffic emissions for the different air pollutants (NOx, PM10, PM2.5, Black Carbon) are reduced in the inner streets of the Neighborhood (blue in Fig. 3). In reality, when a traffic restriction is imposed in a certain zone (e.g. Low Emission Zones), part of the traffic is diverted around it. However, another part of the traffic does not pass close to this area due to several reasons such as people taking very different routes or changing to use public transport. Hence, for some of the scenarios, traffic emissions are increased in the surrounding streets (purple in Fig. 3) to consider the potential traffic diversion. The restrictions of LEZs established in cities are different. Hence, in this study, a wide range of LEZ scenarios is investigated to estimate the potential effects of LEZ with degrees of restrictions and traffic diversion. Five LEZ scenarios (Table 1) are investigated considering two emission reduction factors for LEZ (0.2 and 0.8 times BASE emissions) and three emissions factors for surrounding streets (1, 1.2 and 1.8 times BASE emissions).

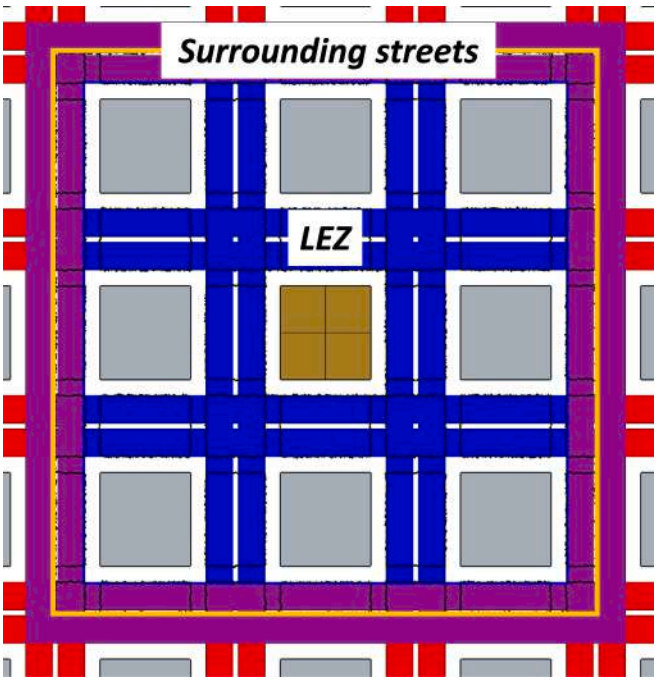


**Fig. 3.** Layout of LEZ scenarios. Blue indicates the emission reductions in the LEZ and purple the emissions in the streets surrounding the LEZ (which may be increased for some scenarios).

- *Green infrastructure (GI)*. Different types of GI composed by different combinations of street trees and hedgerows in the sidewalks and in the middle of the avenues (median strip) were implemented in the central area of the neighborhood. These configurations included

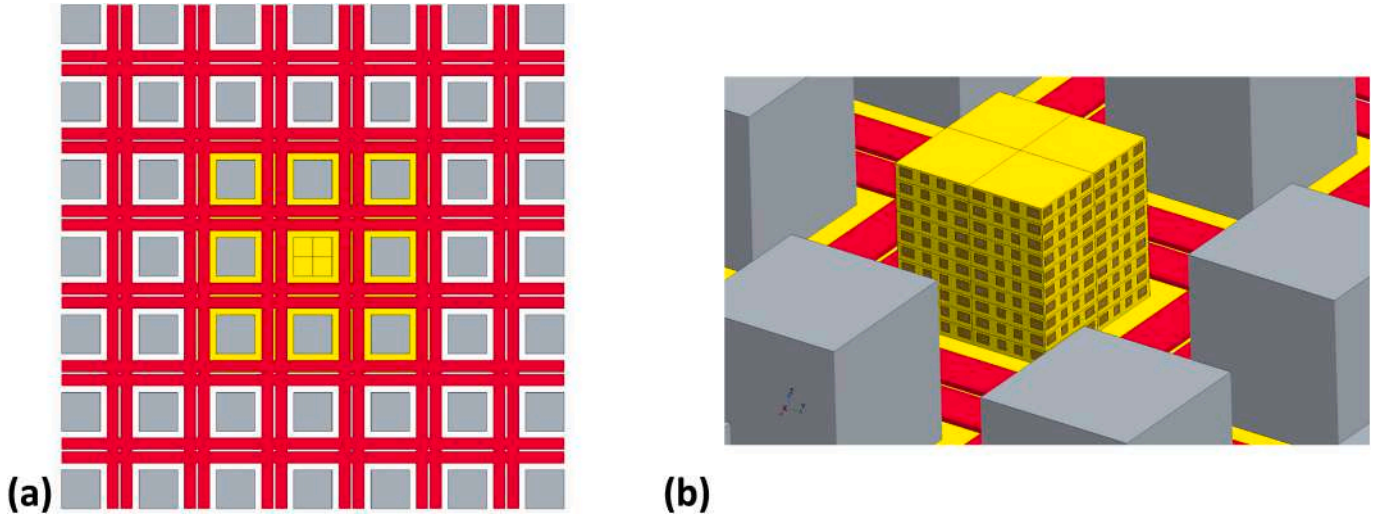


**Fig. 2.** Layout of the area where the photocatalytic materials are implemented (in yellow) (*Photocat_GWR scenario*). (a) plan view, (b) details of the central building. Red indicates the traffic emissions.

**Table 1**
Description of LEZ scenarios.

| Scenario | LEZ emissions | Emissions for streets that surround LEZ |
|---|---|---|
| *LEZ_0.2 + SurroundLEZ_1.0* | *0.2 • BASE Emissions* | *1.0 • BASE Emissions* |
| *LEZ_0.2 + SurroundLEZ_1.2* | *0.2 • BASE Emissions* | *1.2 • BASE Emissions* |
| *LEZ_0.2 + SurroundLEZ_1.8* | *0.2 • BASE Emissions* | *1.8 • BASE Emissions* |
| *LEZ_0.8 + SurroundLEZ_1.0* | *0.8 • BASE Emissions* | *1.0 • BASE Emissions* |
| *LEZ_0.8 + SurroundLEZ_1.2* | *0.8 • BASE Emissions* | *1.2 • BASE Emissions* |

trees and hedgerows located in different configurations, different heights of trees and scenarios with and without green walls and green roofs. The total number of scenarios was 19 and a detailed study of the impact of these GI scenarios on traffic-related air pollutant concentrations were done by Santiago et al. (2022d), while, in this paper, the results corresponding to these scenarios are summarized focusing on two scenarios with different characteristics, which are also combined with LEZ measures. These two scenarios (Fig. 4) are:

- *VEG* (*VEG_1* scenario in Santiago et al. (2022d)), considering 15 m-height trees in the sidewalks and hedgerows in the median strip.
- *VEG_TreesMedian* (*VEG_3* scenario in Santiago et al. (2022d)), considering 15 m-height trees in the sidewalks and in the median strip, as well as hedgerows in the median strip.

The crown is defined considering some real limitations of planting trees in streets (distance from façades, distance between trunks, no invasion of the road, etc.). The horizontal size of the crown is set to 6 m, and covering a vertical distance from 4 m-height to the tree height. The separation between trunks is set to 6 m and the distance between the crown and the building walls is set to 0.5 m. The hedgerows are 1.5 m-height and 2 m-width. The leaf area density (LAD) considered for trees is 0.5 $m^2\ m^{-3}$ (value within the range of LAD of typical urban trees (Abhijith et al., 2017; Buccolieri et al., 2018a)) and 4 $m^2\ m^{-3}$ for hedgerows (Abhijith et al., 2017; Santiago et al., 2019b). In addition, GI scenarios with three different deposition velocities (0, 0.01 and 0.05 m $s^{-1}$) are simulated to investigate the relative contribution of aerodynamic and deposition effects. Deposition velocities depend on the type of pollutant and plant species. The values usually employed in CFD simulations ranges from 0.002 to 0.05 m $s^{-1}$ (Buccolieri et al., 2018a, 2018b). The purpose of this study is not to model specific species of trees, hedgerows and green walls/roofs, and typical values of deposition velocities (0, 0.01 and 0.05 m $s^{-1}$) are used. It could be a typical specie in the city such as *Platanus x Acerifolia*. The modelling of the vegetation effects is described in the Section 2.2.

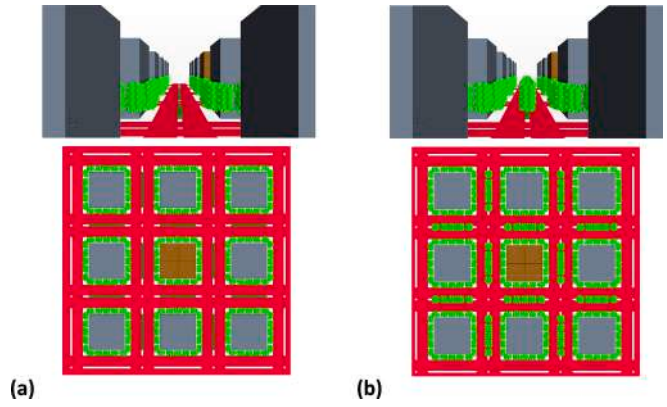


**Fig. 4.** (a) *VEG* scenario (Top: side view; Bottom: top view). (b) *VEG_TreesMedian* scenario (Top panel: side view; Bottom panel: top view).

- *Combinations of LEZ and GI*. Both GI scenarios (*VEG* and *VEG_TreesMedian*) are implanted in the LEZ scenarios previously described. 10 scenarios are simulated (2 GI × 5 LEZ). In addition, for each scenario, three distinct deposition velocities (0, 0.01 and 0.05 m $s^{-1}$) are also investigated.

### 2.2. CFD modelling set-up

All scenarios are simulated through CFD modelling for two wind directions (0° and 45°, Fig. 1). CFD modelling is based on Reynolds-averaged Navier-Stokes (RANS) equations with *Realizable k-ε* turbulent closure, where $k$ is the turbulent kinetic energy and $\varepsilon$ is its dissipation rate. The equations are solved with the software STAR-CCM+ version 15.04.010 from Siemens. This study is focused on traffic-related air pollutants and only traffic emissions, located along the streets, are considered. Two roads of 3 lanes are modelled in each street (red in Fig. 1). Air pollutants emitted by traffic considered non-reactive, such as NOx, PM10, PM2.5 and Black Carbon, are studied, and transport equations of passive scalars are used to simulate its dispersion. Aerodynamic effects for these pollutants are similar, however, the deposition velocity due to the presence of vegetation is different, and in particular is greater for particulate matter (PM10, PM2.5, Black Carbon) than for NOx. In this study, three different deposition velocities (0, 0.01 and 0.05 m $s^{-1}$) are simulated. The aerodynamic effects of vegetation are modelled through sink/source terms in the momentum ($S_{ui}$) and turbulence equations ($S_k$, $S_\varepsilon$) and the dry deposition through a mass sink ($S_d$) in the air pollutant transport equations (Buccolieri et al., 2018a, 2018b). These terms are defined as:

$$Su_i = -\rho LAD c_d U u_i, \tag{1}$$

$$S_k = \rho LAD c_d \left(\beta_p U^3 - \beta_d U k\right), \tag{2}$$

$$S_\varepsilon = \rho LAD c_d \left(C_{\varepsilon 4}\beta_p \frac{\varepsilon}{k} U^3 - C_{\varepsilon 5}\beta_d U \varepsilon\right), \tag{3}$$

where $\rho$ is the air density, $c_d$ the sectional drag coefficient for vegetation (0.2), $U$ the wind speed, and $u_i$ the velocity component in direction $i$. $\beta_p$ is the fraction of mean kinetic energy converted into turbulent kinetic energy, $\beta_d$ the dimensionless coefficient for the short-circuiting of turbulent cascade and $C_{\varepsilon 4}$ and $C_{\varepsilon 5}$ model constants. $\beta_d$, $C_{\varepsilon 4}$ and $C_{\varepsilon 5}$ are based on analytical expressions of Sanz (2003) with $\beta_p = 1$ (Krayenhoff et al., 2015; Santiago et al., 2017a, 2017b, 2022d).

$$S_d = -LAD\ V_{dep} C(x,y,z), \tag{4}$$

where $V_{dep}$ is deposition velocity and C(x,y,z) is the concentration of air pollutant at vegetation location (x,y,z). It is noteworthy that all of these terms are proportional to LAD. Deposition velocity mainly depends on the type of air pollutant and vegetation specie. Many discrepancies of its value have been found in the literature, specifically in urban environments (Buccolieri et al., 2018a, 2018b). and, in this study, three different deposition velocities (0, 0.01 and 0.05 m $s^{-1}$) within the range of published values are used. It is assumed that the results for deposition velocity of 0.01 m $s^{-1}$ are for NOx and 0.05 m $s^{-1}$ for PM10, PM2.5 and Black Carbon, although, considering the discrepancies in the literature (Buccolieri et al., 2018a, 2018b), the values of deposition velocity for each studied pollutant could range from 0.01 to 0.05 m $s^{-1}$. The value of 0 m $s^{-1}$ means that there is no deposition. This approach allows investigating the relative contribution of aerodynamic and deposition effects to the net effect of GI on air quality.

Numerical domain is built taking into account the best practice guidelines of COST Action 732 for CFD simulations (Franke et al., 2007;

Di Sabatino et al., 2011). The height of the domain is defined as 11 times the height of the buildings and the distance between the lateral domain boundaries and the obstacles is set as 15 times the height of the buildings. An irregular polyhedral mesh with hexahedral cells close to ground, emissions and obstacle was used to discretize the numerical domain. A spatial resolution of 2.5 m inside the array of buildings is considered with refinements of 0.5 m close to obstacles and emissions. The total number of cells is $11.5 \times 10^6$. A grid sensitivity test is carried out using three grids with different spatial resolution. The coarse, medium and fine grids present refinements of 0.75, 0.5 and 0.25 m close to obstacles and a total number of cells of $8.3 \times 10^6$, $11.5 \times 10^6$ and $30.7 \times 10^6$, respectively. BASE scenario for a wind direction of 0° is simulated. Streamwise velocity, vertical velocity and turbulent kinetic energy obtained for the three grids are compared. Results are similar being selected the medium grid as a good compromise between accuracy and computational cost. Neutral profiles of wind speed, turbulent kinetic energy and $\varepsilon$ are imposed at inlet boundaries (Eqs. (5)–(7)) (Richards and Hoxey, 1993). For air pollutant concentration, a value of zero is imposed at these boundaries since only local traffic emissions are taken into account. Building surfaces are considered as smooth walls and ground as a wall with a roughness of $z_0 = 0.03$ m. At the top of the domain, symmetry conditions are imposed (zero normal velocity and zero gradients of all variables).

$$u(z) = \frac{u_*}{\kappa} ln\left(\frac{z + z_0}{z_0}\right), \tag{5}$$

$$k = \frac{u_*^2}{\sqrt{C_\mu}}, \tag{6}$$

$$\varepsilon = \frac{u_*^3}{\kappa(z + z_0)}, \tag{7}$$

where $u_*$ is the friction velocity and $\kappa$ is von Karman's constant (0.4). These profiles are widely used in CFD simulation over urban environments (Buccolieri et al., 2011; Santiago et al., 2017a, 2017c). Friction velocity is set to $u_* = 0.22$ m s$^{-1}$, so inlet wind speed at 10 m is 3.2 m s$^{-1}$, which is similar to the inlet wind speed used in other studies over real urban environment (Santiago et al., 2017c; Sanchez et al., 2017; Rivas et al., 2019). More details about CFD modelling set-up and the grid sensitivity test can be found in Santiago et al. (2022d).

Model evaluation was performed in Santiago et al. (2022d) and, in the present paper, a summary of the previous results is presented. Wind flow around the buildings was evaluated for the BASE scenario comparing vertical profiles of modelled streamwise velocity ($U$), vertical velocity ($W$) and turbulent kinetic energy ($k$) at several locations with wind-tunnel data. A good agreement was found. In addition, statistical metrics (NMSE, FB, FAC2 and R) were computed for $U$, $W$ and $k$. Correlation (R) was high ($> 0.85$ for $U$, $W$ and $k$) and NMSE was 0.04, 0.11 and 0.19 for $U$, $W$ and $k$, respectively and FB was 0.13, 0.04 and 0.36 for $U$, $W$ and $k$, respectively and FAC2 for $k$ was 0.83. Therefore, NMSE and FB were low, except FB for $k$. This statistical analysis revealed a suitable model performance with only a slight underestimation of turbulent kinetic energy due to some discrepancies between model set-up and wind-tunnel configuration. Experimental data for the same GI scenarios studied were not available, therefore vegetation modelling could not be evaluated using these scenarios. However, the same vegetation model was previously validated in several studies (Krayenhoff et al., 2015; Santiago et al., 2017b, 2017c, 2019b), applied to both simplified and real urban environments. In addition, previous studies in real environments with urban GI (Santiago et al., 2013, 2017a, 2020; Sanchez et al., 2017) appropriately modelled air pollutant concentrations (NOx, $NO_2$, $PM_{10}$) using the same vegetation modelling approach.

The impacts of air pollution mitigation measures are assessed by comparing concentrations for each measure with the BASE scenario. The modelled concentration is normalized as follows:

$$C_{norm}(x, y, z) = \frac{C(x, y, z)u_*}{Q,} \tag{8}$$

where $Q$ is the emission rate of traffic-related air pollutant in kg m$^{-2}$ s$^{-1}$. Air pollutant concentrations at pedestrian level (3 m-height) is used for analysis due to the study focuses on population exposure. At this height, the spatial variability of air pollutant concentrations in the streets and the spatially-averaged concentrations in several horizontal sections are investigated. The spatially-averaged concentrations are computed over horizontal sections covering:

- the whole area where the measures are implanted (*Neighborhood*);
- sidewalks and crosswalk of the neighborhood (*Sidewalks*);
- only the sidewalks around the central building (*Building*);

In addition, for LEZ scenarios, the spatially-averaged concentrations are also averaged for:

- the area that surrounds the neighborhood (*Surrounding*);
- the total area that covers *Neighborhood* and *Surrounding* (*Neighborhood + Surrounding*).

## 3. Results and discussion

In this section, firstly, the effects of each single measure on air pollutant concentrations at pedestrian level are investigated to compare their effectiveness. The effects of photocatalytic materials, LEZ and GI are discussed in Sections 3.1, 3.2 and 3.3, respectively. Then, the effects of combining GI and LEZ are assessed to estimate the air quality improvements provided by this combination (Section 3.4). The criterion of effectiveness is based on the comparison between the spatially-averaged concentrations at pedestrian level over different areas (*Building*, *Sidewalks* and *Neighborhood*) for each scenario and the results for the BASE case. In addition, maps of concentration at pedestrian level are also analyzed due to the fact that the effects of each measure is very heterogeneous at pedestrian level.

### 3.1. Effects of photocatalytic materials on pedestrian level concentrations

Firstly, it is noteworthy that photocatalytic materials, activated by UV solar radiation, react with nitrogen oxides (NOx), sulfur oxides (SOx) and organic substances present in the atmosphere, also in the form of atmospheric particulate matter (PM), producing inert particles that adhere to the wall with the photocatalytic materials (Pulvirenti et al., 2020). Photocatalytic coatings are mainly used for the reduction of NOx due to the NO photocatalytic absorption. In this paper, for simplicity, the photocatalytic effects on NOx are modelled through a NOx deposition velocity and the effects on particulate matter concentrations are assumed negligible.. The spatially-averaged concentrations at pedestrian level for *Photocat_G* and *Photocat_GWR* scenarios are computed over different areas (*Building*, *Sidewalks* and *Neighborhood*) for both wind directions, and the variation of these values with respect to the BASE scenarios are showed in Table 2. Higher concentration reductions are found close to the central building (*Building*) and for the 45° wind direction, although reductions are small (lower than 4 %) for all scenarios. This fact is due to the reduction of concentrations is limited to nearby areas to surfaces where photocatalytic materials are implemented. This agrees with previous studies (Fernández-Pampillón et al., 2021; Sanchez et al., 2021). In Fernández-Pampillón et al. (2021), focused on field experiments in a real urban environment, no significant improvement in air quality was found near the road where a photocatalytic material was applied. Furthermore, Sanchez et al. (2021) estimated reductions below 2 % of $NO_2$ concentrations from numerical simulations for a real urban scenario considering the photocatalytic area applied to an entire neighborhood. Pulvirenti et al. (2020) obtained higher efficiency for NO

**Table 2**
Single measures scenarios: variations of the spatially-averaged concentrations compared with BASE scenarios over different areas (*Building, Sidewalks, Neighborhood, Surrounding and Neighborhood + Surrounding*) at pedestrian level for 0° and 45° wind directions (in %). The two values indicate the best and the worst effectiveness of each measure. *Photocat* includes *Photocat_G* and *Photocat_GWR* scenarios; *LEZ_0.2* includes *LEZ_0.2 + SurroundLEZ_1.0*, *LEZ_0.2 + SurroundLEZ_1.2*, and *LEZ_0.2 + SurroundLEZ_1.8* scenarios; and *LEZ_0.8* includes *LEZ_0.8 + SurroundLEZ_1.0* and *LEZ_0.8 + SurroundLEZ_1.2*.

| | Building | Sidewalks | Neighborhood | Surrounding | Neighborhood + Surrounding |
|---|---|---|---|---|---|
| *Photocat* | −3.8 % | −2.1 % | −1.9 % | – | – |
| | −1.9 % | −1.5 % | −1.2 % | | |
| *LEZ_0.2* | −61 % | −41 % | −41 % | −7 % | −17 % |
| | −52 % | −14 % | −14 % | 15 % | 4 % |
| *LEZ_0.8* | −15 % | −10 % | −10 % | −2 % | −5 % |
| | −13 % | −4 % | −3 % | 4 % | 1 % |
| *VEG* | −4 % | 3 % | −4 % | – | – |
| *(NO Deposition)* | 6 % | 8 % | 7 % | | |
| *VEG* | −11 % | −2 % | −9 % | – | – |
| *(Vdep = 0.01 m s$^{-1}$)* | −3 % | 1 % | 1 % | | |
| *VEG* | −27 % | −16 % | −21 % | – | – |
| *(Vdep = 0.05 m s$^{-1}$)* | −26 % | −15 % | −12 % | | |
| *VEG_TreesMedian* | 6 % | 12 % | 4 % | – | – |
| *(NO Deposition)* | 36 % | 23 % | 25 % | | |
| *VEG_TreesMedian* | −3 % | 5 % | −2 % | – | – |
| *(Vdep = 0.01 m s$^{-1}$)* | 18 % | 13 % | 16 % | | |
| *VEG_TreesMedian* | −24 % | −13 % | −18 % | – | – |
| *(Vdep = 0.05 m s$^{-1}$)* | −20 % | −9 % | −5 % | | |

up to 40–50 % but limited to a volume close to the coated walls.

### 3.2. Effects of LEZ on pedestrian level concentrations

The spatially-averaged concentrations at pedestrian level for each LEZ scenario are computed over *Building*, *Sidewalks*, *Neighborhood, Surrounding and Neighborhood + Surrounding* for both wind directions. Differences with the BASE scenarios are shown in Tables 2 and Appendix B. However, the effects are spatially heterogeneous and maps of $C_{norm}$ at 3 m-height for the LEZ scenarios are shown in Fig. 5.

In these scenarios, the effectiveness of LEZ is determined by two main factors: the intensity of LEZ restriction and the intensity of traffic diversion. For the most restricted LEZ without traffic diversion (*LEZ_0.2 + SurroundLEZ_1.0*), the reduction of traffic-related air pollutant concentrations at pedestrian level is the highest obtained for the single measures investigated with 59 % and 61 % for 0° and 45° wind direction, respectively. Only in the scenarios with strong traffic diversion and 0° wind direction, the spatially-averaged concentrations including the neighborhood and surrounding streets increase slightly (4 % and 1 % for LEZ_0.2 + SurroundLEZ_1.8 and LEZ_0.8 + SurroundLEZ_1.2, respectively). It means that the increase in air pollutant concentration in surrounding areas is slightly higher than the decrease in the LEZ (Fig. 5). However, for most scenarios and conditions, this single measure is very effective in reducing air pollution levels. The variation of spatially-averaged concentrations at pedestrian level compared with the BASE scenario ranges from −61 % to −13 % for *Building* area, from −41 % to −4 % for *Sidewalks* area, from −41 % to −3 % for *Neighborhood* area, from −7 % to 15 % for *Surrounding* area and from −21 % to 0 for *Neighborhood + Surrounding* area.

To investigate the effects on the spatial distribution of air pollutant concentrations, firstly it is analyzed the concentration maps for the BASE case and the processes involved in the dispersion. The interaction of atmosphere with urban obstacles induces complex wind flow patterns in the street which drives the pollutant dispersion. For 0° case, the wind flow is orthogonal to the street canyons in Y-direction and there is a vertical clockwise vortex in the middle of the canyon (not shown here). This is in agreement with the skimming flow regime defined by Oke (1988) for street canyons with aspect ratio H/W = 1. The center of the vortex is displaced to the center of the street canyon due to, in this case, the street canyon is not two-dimensional. A similar vortex shape was also found by Brown et al. (2001) in wind-tunnel experiments and Lien and Yee (2004) and Santiago et al. (2007) in modelling studies. At pedestrian level, this vortex induces higher concentrations at the leeward wall of buildings than at the windward wall (Fig. 5). Similar pollutant distributions were found in other studies (Santiago et al., 2007; Angelidis et al., 2012; Martilli et al., 2015). In the bottom part of the streets (e.g., at pedestrian level), a flow out of the canyon laterally and towards the leeward wall is produced by the divergence close to the ground of the downward wind flow at the windward face of the building. This flow pattern produces the highest pollutant concentration outside the canyon (i.e. in the streets parallel to the inlet wind direction) (Santiago et al., 2007). For 45°, the pollutant distribution at pedestrian level is different. Maximum concentrations are found close to both leeward façades of buildings. This fact is due to the horizontal vortices around the buildings. A similar wind flow pattern was found in previous studies (Claus et al., 2012; Coceal et al., 2014). The pollutants accumulate in the wakes produced by the buildings in both leeward facades. For LEZ scenarios, the pollutant emissions change, but the wind flow is not modified in comparison with the BASE case. Hence, the shape of the distribution of air pollutant concentrations is similar to the BASE case for the same wind direction, but with different concentration levels. Concentrations are notably reduced in the *Neighborhood*, but increase in the surrounding streets when the traffic diversion is strong.

### 3.3. Effects of GI on pedestrian level concentrations

Santiago et al. (2022d) investigated the impact of 19 GI scenarios on traffic-related air pollutant concentrations in this idealized urban environment. In general, the main effects of GI are:

- Reducing the street ventilation in the area where GI is implemented, and consequently inducing an increase in concentration.
- Acting as a barrier for air pollutants emitted outside this area.
- Removing air pollutant from air by means of dry deposition.

It is assumed that the results for deposition velocity of 0.01 m s$^{-1}$ are for NOx and 0.05 m s$^{-1}$ for PM10, PM2.5, and Black Carbon, although, considering the discrepancies in the literature, the values of deposition velocity for each studied pollutant could range from 0.01 to 0.05 m s$^{-1}$. In the present paper, the results corresponding to one scenario with trees in the median street (*VEG_TreesMedian*) and other with trees in the sidewalks (*VEG*) are analyzed in detail. Both scenarios are also combined with LEZ scenarios in Section 3.4. The variation of spatially-averaged concentrations at pedestrian level for both GI scenarios compared to the BASE case is computed over *Building*, *Sidewalks* and *Neighborhood* for both wind directions (Table 2 and Appendix B). In addition, maps of

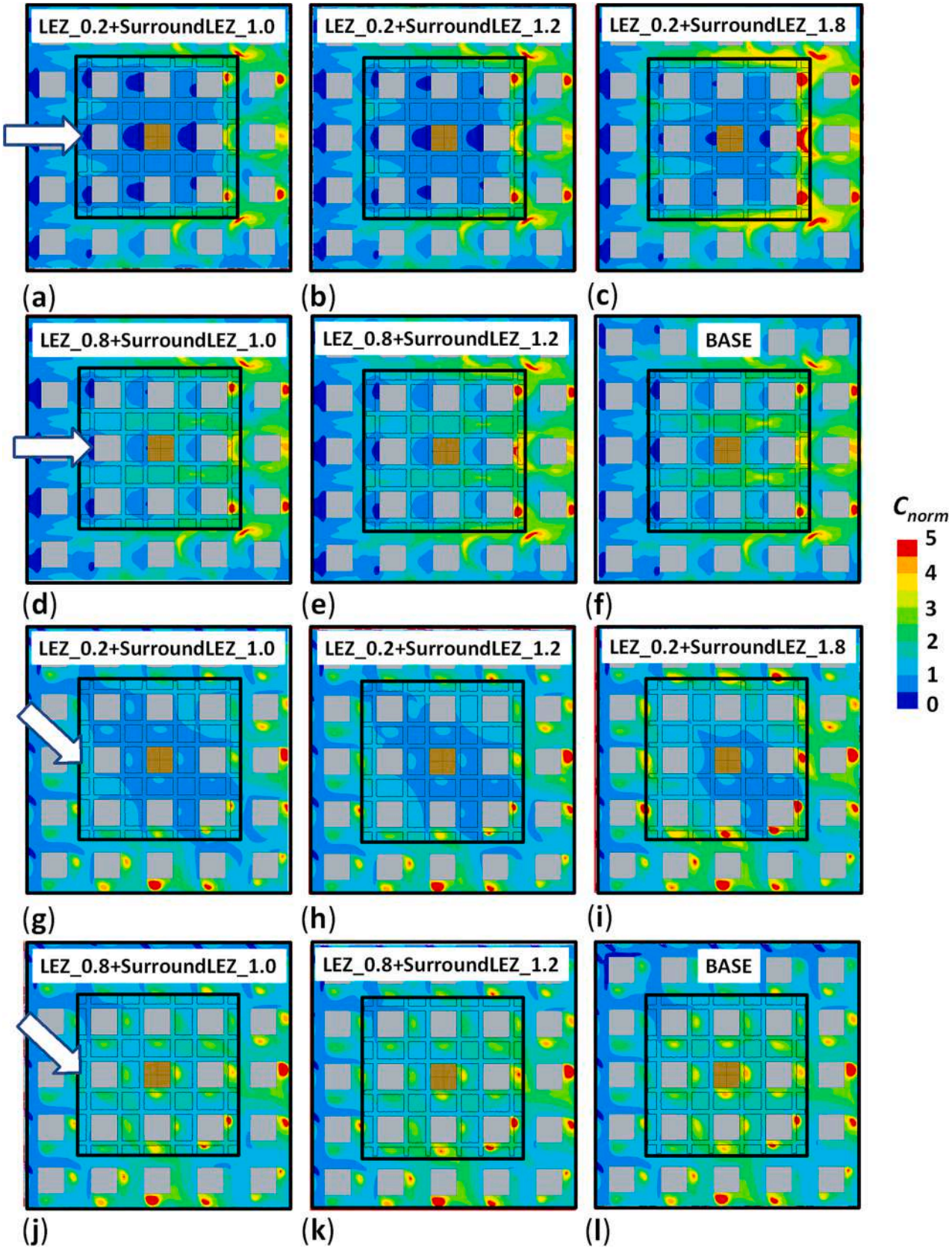


**Fig. 5.** LEZ scenarios: maps of Cnorm at 3 m-height for both wind directions. For 0° wind direction: (a) LEZ_0.2 + SurroundLEZ_1.0 scenario; (b) LEZ_0.2 + SurroundLEZ_1.2 scenario; (c) LEZ_0.2 + SurroundLEZ_1.8 scenario; (d) LEZ_0.8 + SurroundLEZ_1.0 scenario; (e) LEZ_0.8 + SurroundLEZ_1.2 scenario; (f) BASE scenario. For 45° wind direction: (g) LEZ_0.2 + SurroundLEZ_1.0 scenario; (h) LEZ_0.2 + SurroundLEZ_1.2 scenario; (i) LEZ_0.2 + SurroundLEZ_1.8 scenario; (j) LEZ_0.8 + SurroundLEZ_1.0 scenario; (k) LEZ_0.8 + SurroundLEZ_1.2 scenario; (l) BASE scenario.

$C_{norm}$ at 3 m-height for the GI scenarios investigated (Fig. 6) are estimated in order to study the spatial variability.

For these scenarios, the wind flow, and, consequently, the air pollutant dispersion, are modified in comparison with the BASE case. In Fig. 6, it is also observed that the effects of GI are spatially heterogeneous. Even in cases with spatially-averaged concentrations lower than that obtained for the *BASE* scenarios, there are zones where the concentrations increase with respect to the *BASE* case. For 0° wind direction, trees in the median strip (*VEG_TreesMedian* scenario) weaken the ventilation in the streets where maximum concentrations are found in the BASE case. This fact induces an important increase in concentrations, in particular, in these streets parallel to the wind direction (Fig. 6). It is observed that close to the median strip the ventilation is reduced accumulating air pollutant there. In this area, air pollutant concentrations are larger than those obtained for the BASE scenarios, even for the cases with $V_{dep} = 0.05$ m s$^{-1}$ where the spatially-averaged concentrations decreases. This fact induces that the spatially-averaged concentrations over *Building*, *Sidewalks* and *Neighborhood* increase 36 %, 23 % and 25 % respectively for NO deposition scenarios and increase 18 %, 13 % and 16 % respectively for $V_{dep} = 0.01$ m s$^{-1}$ scenarios (Table 2 and Appendix B). For VEG scenario, the reduction of street ventilation due to aerodynamic effects is smaller than for *VEG_TreesMedian* scenario. Hence, for $V_{dep} = 0.01$ m s$^{-1}$ the increase of spatially-averaged concentrations over *Building*, *Sidewalks* and *Neighborhood* is negligible. For the 45° wind direction, the aerodynamic effects are less relevant than for 0° wind direction. This is due to wind flow and air pollutant dispersion within the streets for this inlet wind directions. The reduction of street ventilation by the trees in the median strip is not so large than for 0°. *VEG* scenarios (trees only in the sidewalks) are more effective for air pollutant concentration reductions (Table 2 and Appendix B). This is due to trees in the sidewalks seem to be act as a barrier for the air pollutant emitted outside the central area reducing air pollutant concentration in the central area of the domain. In addition, the horizontal vortices around the buildings where the pollutants were accumulated close to leeward façade for the BASE case, are modified by the presence of trees in the sidewalks, and hence, the concentrations are reduced, in particular when deposition is considered. Considering the highest deposition case, the spatially-averaged concentrations decrease for both scenarios (Table 2 and Appendix B). In general, the reductions compared with the *BASE* case are lower than for most of LEZ scenarios although much

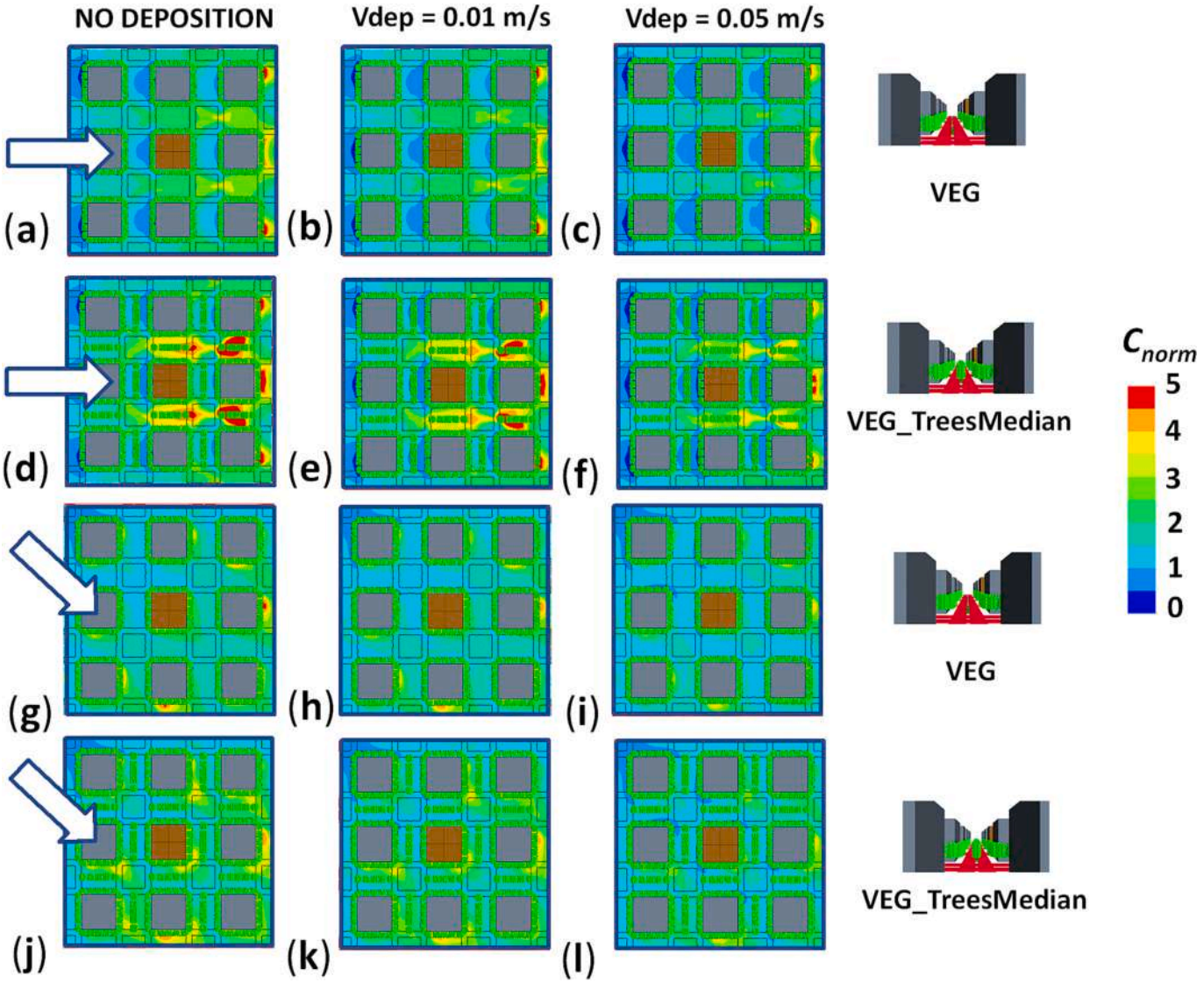


**Fig. 6.** GI scenarios: maps of $C_{norm}$ at 3 m-height. (a) *VEG* scenario without deposition for 0° wind direction. (b) Same as (a) but with $V_{dep} = 0.01$ m s$^{-1}$. (c) Same as (a) but with $V_{dep} = 0.05$ m s$^{-1}$. (d) *VEG_TreesMedian* scenario without deposition for 0° wind direction. (e) Same as (d) but with $V_{dep} = 0.01$ m s$^{-1}$. (f) Same as (d) but with $V_{dep} = 0.05$ m s$^{-1}$. (g) *VEG* scenario without deposition for 45° wind direction. (h) Same as (g) but with $V_{dep} = 0.01$ m s$^{-1}$. (i) Same as (g) but with $V_{dep} = 0.05$ m s$^{-1}$. (j) *VEG_TreesMedian* scenario without deposition for 45° wind direction. (k) Same as (j) but with $V_{dep} = 0.01$ m s$^{-1}$. (l) Same as (j) but with $V_{dep} = 0.05$ m s$^{-1}$.

higher than for photocatalytic materials scenarios. The maximum reduction of spatially-averaged concentrations is obtained for *VEG* scenario with $V_{dep} = 0.5$ m s$^{-1}$ (26 %, 15 % and 12 % over *Building*, *Sidewalks* and *Neighborhood* for 0° wind direction and 27 %, 16 % and 21 % over *Building*, *Sidewalks* and *Neighborhood* for 45° wind direction). In general, the aerodynamic effects of street trees tend to increase air pollutant concentrations at pedestrian level. This is in agreement with previous studies (e.g., Vos et al., 2013; Gromke and Blocken, 2015; Jeanjean et al., 2017a; Kumar et al., 2019; Tomson et al., 2021) that found this increase of concentration in particular for streets with low aspect ratio like the streets of this study with H/W = 1.

### 3.4. Effects of combined measures (LEZ + GI) on pedestrian level concentrations

The following scenarios combine traffic emission reductions (LEZ scenarios) with the implementation of GI in the central part of the domain. Therefore, ten scenarios are investigated combining LEZ and GI and for each GI three different deposition velocities are also considered. Simulations for each deposition velocity correspond to results for different conditions. It is difficult to determine the correspondence between deposition velocity, plant species, and pollutants due to the discrepancies between deposition velocities found in the literature (Buccolieri et al., 2018a, 2018b). In this study, three different deposition velocities (0, 0.01, and 0.05 m s$^{-1}$) are simulated to provide results within a realistic range of conditions. As previously commented, it is assumed that the results for deposition velocity of 0.01 m s$^{-1}$ are for NOx and 0.05 m s$^{-1}$ for PM10, PM2.5, and Black Carbon, although, considering the discrepancies in the literature, the values of deposition velocity for each studied pollutant could range from 0.01 to 0.05 m s$^{-1}$. For each combined measure, the spatially-averaged concentrations at pedestrian level are computed over *Building*, *Sidewalks*, *Neighborhood, Surrounding and Neighborhood + Surrounding* for both wind directions, and the deviations from the BASE scenario are shown in Table 3 and Appendix B.

For the most restricted LEZ without traffic diversion (*LEZ_02 + SurroundLEZ_1.0*), the implementation of both GI scenarios with the largest deposition velocity provides the highest reduction of concentrations (Table 3 and Appendix B). For *LEZ_02 + SurroundLEZ_1.0* scenario (Table 2 and Appendix B), for 0° wind direction, the reductions of spatially-averaged concentrations are 59 % over *Building* area, 39 % over *Sidewalks*, 39 % over *Neighborhood* and 17 % over *Neighborhood + Surrounding* area. And for 45° wind direction, the reductions are 61 % over *Building* area, 41 % over *Sidewalks*, 41 % over *Neighborhood* and 21 % over *Neighborhood + Surrounding* area. These reductions produced by *LEZ_02 + SurroundLEZ_1.0* enhanced when GI for the largest deposition velocity is implemented. For 0° wind direction, the reduction of spatially-averaged concentrations for *VEG* (*VEG_TreesMedian*) scenario with $V_{dep} = 0.05$ m s$^{-1}$ are 73 % (75 %) over *Building* area, 48 % (46 %) over *Sidewalks*, 46 % (44 %) over *Neighborhood* and 22 % (21 %) over *Neighborhood + Surrounding* area. And for 45° wind direction, these reductions reach 75 % (76 %) over *Building* area, 51 % (51 %) over *Sidewalks*, 53 % (53 %). For *LEZ_02 + SurroundLEZ_1.0 + GI* scenarios with $V_{dep} = 0.01$ m s$^{-1}$, the reductions are similar with (Table 3 and Appendix B) and without GI (Tables 2 and Appendix B). This fact is relevant since the other vegetation ecosystem services can be used without considering the potential air quality problems as long as traffic emissions in the area are reduced. The intensity of the traffic diversion in the streets that surround the LEZ affects air pollutant concentrations (Table 3 and Appendix B). However, only for the scenarios with strong traffic diversion and low deposition conditions, the spatially-averaged concentrations including the neighborhood and the streets that surround the LEZ increase respect to BASE scenario. Similar conclusions can be extracted from *LEZ_0.8 + GI* scenarios (Table 3), with the exception that the reductions are more moderate due to the lower restrictions of LEZ. It is noteworthy to analyze in depth the results for *VEG_TreesMedian* scenario. For 0° wind direction, trees in the median strip weaken the street ventilation inducing an increase of concentrations respect to BASE scenario for this single measure when deposition is low ($V_{dep} = 0.01$ m s$^{-1}$) (e.g., increase of 18 % over *Building* and 16 % over *Neighborhood*, Table 2 and Appendix B). However, when this vegetation configuration is

**Table 3**
LEZ + GI scenarios: variations of the spatially-averaged concentrations compared with BASE scenarios over different areas (*Building, Sidewalks, Neighborhood, Surrounding and Neighborhood + Surrounding*) at pedestrian level for 0° and 45° wind directions (in %). The two values indicate the best and the worst effectiveness of each measure. *LEZ_0.2* includes *LEZ_0.2 + SurroundLEZ_1.0*, *LEZ_0.2 + SurroundLEZ_1.2*, and *LEZ_0.2 + SurroundLEZ_1.8* scenarios; and *LEZ_0.8* includes *LEZ_0.8 + SurroundLEZ_1.0* and *LEZ_0.8 + SurroundLEZ_1.2*.

| | Building | Sidewalks | Neighborhood | Surrounding | Neighborhood + Surrounding |
|---|---|---|---|---|---|
| *LEZ_0.2 +* | −65 % | −40 % | −43 % | −4 % | −20 % |
| *VEG (NO Deposition)* | −50 % | −7 % | −8 % | 16 % | 5 % |
| *LEZ_0.2+* | −68 % | −43 % | −46 % | −5 % | −21 % |
| *VEG* | −55 % | −12 % | −12 % | 13 % | 3 % |
| *(Vdep = 0.01 m s$^{-1}$)* | | | | | |
| *LEZ_0.2+* | −75 % | −51 % | −53 % | −6 % | −25 % |
| *VEG* | −68 % | −25 % | −22 % | 12 % | −2 % |
| *(Vdep = 0.05 m s$^{-1}$)* | | | | | |
| *LEZ_0.2+ VEG_TreesMedian (NO Deposition)* | −63 % | −37 % | −40 % | −1 % | −17 % |
| | −45 % | 1 % | 1 % | 16 % | 9 % |
| *LEZ_0.2+ VEG_TreesMedian (Vdep = 0.01 m s$^{-1}$)* | −67 % | −41 % | −44 % | −2 % | −19 % |
| | −54 % | −6 % | −5 % | 19 % | 6 % |
| *LEZ_0.2+ VEG_TreesMedian (Vdep = 0.05 m s$^{-1}$)* | −76 % | −51 % | −53 % | −6 % | −24 % |
| | −72 % | −22 % | −19 % | 16 % | −1 % |
| *LEZ_0.8+* | −19 % | −8 % | −14 % | −1 % | −5 % |
| *VEG (NO Deposition)* | −8 % | 4 % | 3 % | 6 % | 3 % |
| *LEZ_0.8+* | −25 % | −13 % | −18 % | −2 % | −7 % |
| *VEG* | −16 % | −2 % | −2 % | 5 % | 1 % |
| *(Vdep = 0.01 m s$^{-1}$)* | | | | | |
| *LEZ_0.8+* | −39 % | −25 % | −29 % | −4 % | −13 % |
| *VEG* | −37 % | −18 % | −15 % | 2 % | −6 % |
| *(Vdep = 0.05 m s$^{-1}$)* | | | | | |
| *LEZ_0.8+ VEG_TreesMedian (NO Deposition)* | −12 % | 0 % | −7 % | 4 % | 0 % |
| | 16 % | 17 % | 19 % | 9 % | 9 % |
| *LEZ_0.8+ VEG_TreesMedian (Vdep = 0.01 m s$^{-1}$)* | −19 % | −7 % | −13 % | 3 % | −4 % |
| | 0 % | 8 % | 10 % | 8 % | 5 % |
| *LEZ_0.8+ VEG_TreesMedian (Vdep = 0.05 m s$^{-1}$)* | −37 % | −23 % | −27 % | −5 % | −11 % |
| | −33 % | −13 % | −8 % | 4 % | −4 % |

combined with a reduction of traffic emissions in the same area, spatially-averaged concentrations are reduced in the case of enough emission reductions and low traffic diversion (e.g., *LEZ_0.2 + SurroundLEZ_1.0+ VEG_TreesMedian* (decrease of 60 % over *Building* and 33 % over *Neighborhood*) and *LEZ_0.2 + SurroundLEZ_1.2+ VEG_TreesMedian* (decrease of 58 % over *Building* and 26 % over *Neighborhood*) scenarios, Table 3 and Appendix B).

The concentration variations are also spatially very heterogeneous. Figs. 7 and 8 show the maps of $C_{norm}$ at 3 m-height for *LEZ_0.2 + VEG_TreesMedian* and *LEZ_0.8 + VEG_TreesMedian* for 0° wind direction. The maps for the other scenarios and wind directions are shown in Appendix A. For all scenarios, in cases with traffic diversion, concentrations increase respect to the BASE scenario in the streets that surround the LEZ. Larger the intensity of traffic diversion larger the concentrations increase. Within LEZ, the traffic emission reductions induce concentration reductions (larger traffic restrictions larger concentration reductions). The effects of GI are more complex since the wind flow is modified as explained in previous section. In the zone where vegetation is implanted, ventilation of these streets is reduced. For example, for *VEG_TreesMedian* scenarios and 0° wind direction, ventilation is reduced in the street parallel to the wind direction (Figs. 6d-6f, 7 and 8) and concentrations increases respect to the BASE case (Fig. 5f). However, the concentration increase due to this effect is balanced by emission reductions of LEZ. The effects of strong traffic restrictions (*LEZ_0.2* scenarios) are more important than the impact of the street ventilation reduction induced by trees in the median strip (Fig. 7). However, for *LEZ_08* scenarios (Fig. 8), the reduction of emissions is not enough to obtain a decrease of total concentrations respect to the BASE scenario. In general, for all scenarios and conditions, traffic emission reductions reduce the negative effects of vegetation (ventilation reduction) on air pollutant concentrations. For VEG scenarios (trees only in the sidewalks) (Appendix A), the conclusions are similar but the reduction of concentrations are more important. In addition, deposition and barrier effects for air pollutant emitted outside the center of the domain helps to improve air quality inside the neighborhood being the combination of a very restrictive LEZ and GI (for this urban

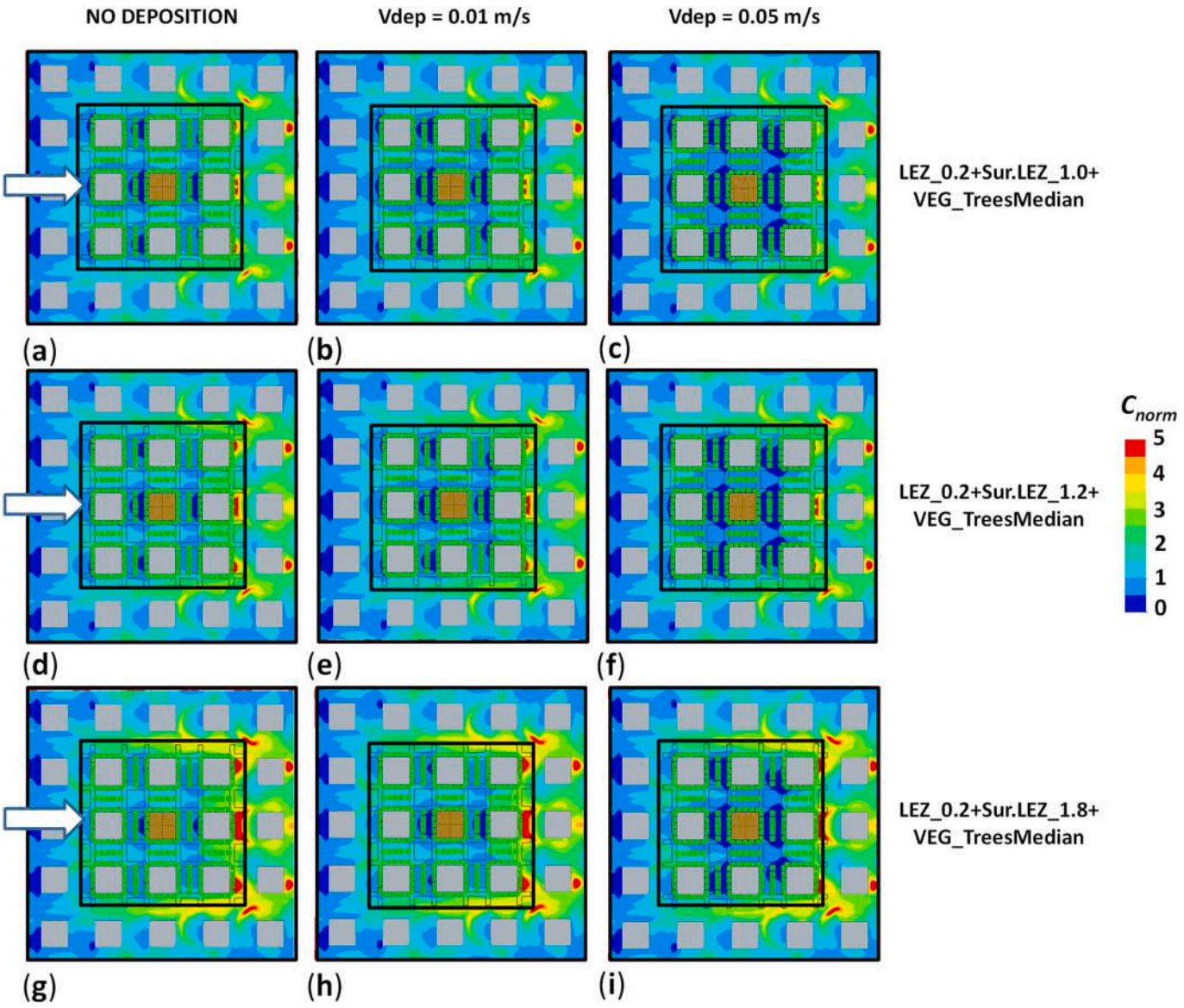


**Fig. 7.** *LEZ_0.2* scenarios with GI (VEG_TreesMedian): maps of $C_{norm}$ at 3 m-height. (a) *LEZ_0.2 + SurroundLEZ_1.0 + VEG_TreesMedian* scenario without deposition for 0° wind direction. (b) Same as (a) but with $V_{dep} = 0.01$ m s$^{-1}$. (c) Same as (a) but with $V_{dep} = 0.05$ m s$^{-1}$. (d) *LEZ_0.2 + SurroundLEZ_1.2 + VEG_TreesMedian* scenario without deposition for 0° wind direction. (e) Same as (d) but with $V_{dep} = 0.01$ m s$^{-1}$. (f) Same as (d) but with $V_{dep} = 0.05$ m s$^{-1}$. (g) *LEZ_0.2 + SurroundLEZ_1.8 + VEG_TreesMedian* scenario without deposition for 0° wind direction. (h) Same as (g) but with $V_{dep} = 0.01$ m s$^{-1}$. (i) Same as (g) but with $V_{dep} = 0.05$ m s$^{-1}$.

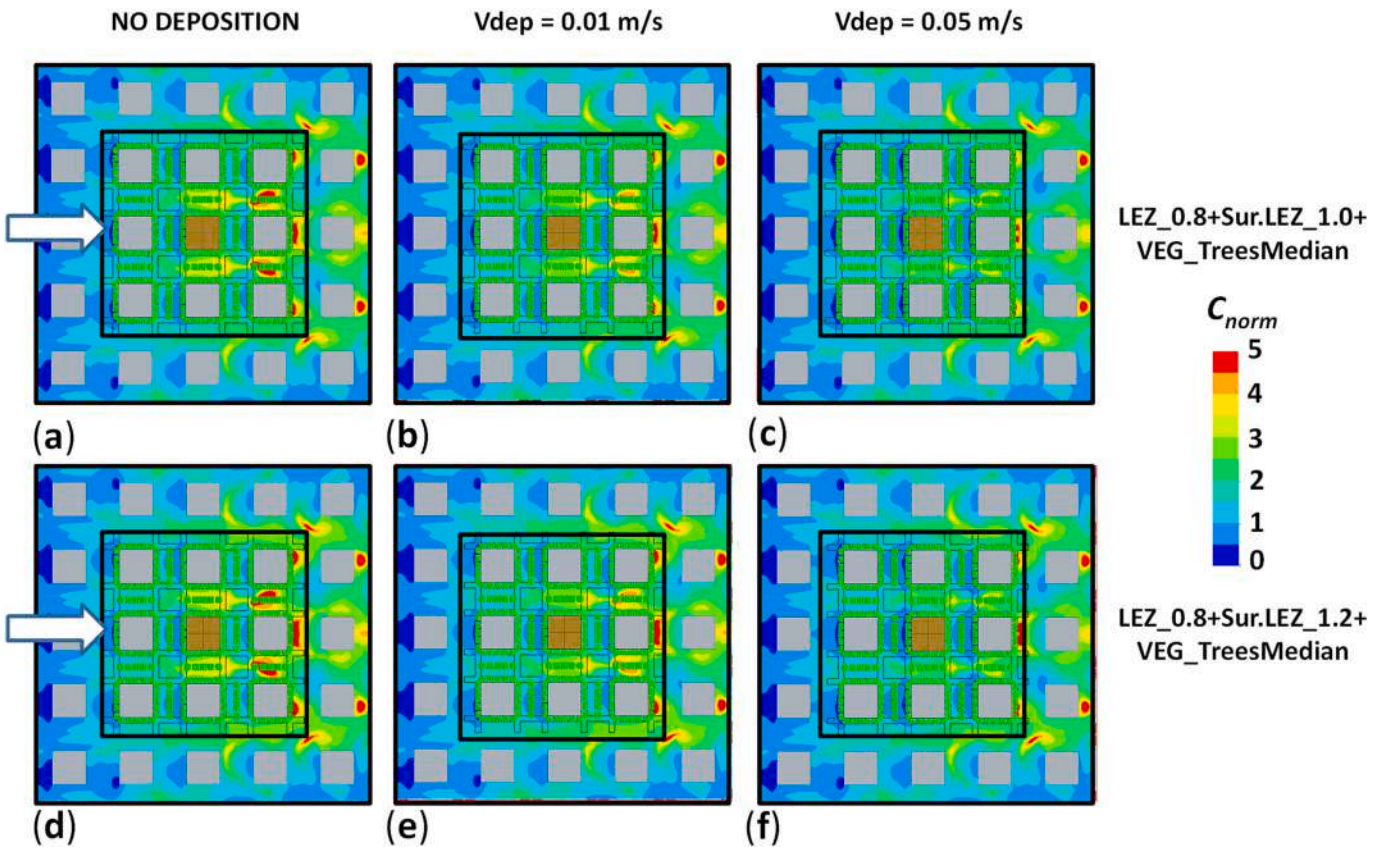


**Fig. 8.** *LEZ_0.8* scenarios with GI (VEG_TreesMedian): maps of $C_{norm}$ at 3 m-height. (a) *LEZ_0.8 + SurroundLEZ_1.0 + VEG_TreesMedian* scenario without deposition for 0° wind direction. (b) Same as (a) but with $V_{dep} = 0.01$ m s$^{-1}$. (c) Same as (a) but with $V_{dep} = 0.05$ m s$^{-1}$. (d) *LEZ_0.8 + SurroundLEZ_1.2 + VEG_TreesMedian* scenario without deposition for 0° wind direction. (e) Same as (d) but with $V_{dep} = 0.01$ m s$^{-1}$. (f) Same as (d) but with $V_{dep} = 0.05$ m s$^{-1}$.

configurations with trees only in the sidewalks) better than any single measure, in particular for large deposition scenarios.

## 4. Summary and conclusions

The present paper investigates the impact of different local air pollution mitigation measures on traffic-related air pollutant concentrations at pedestrian level in the same urban-like environment. Several individual mitigation measures such as LEZ, GI and photocatalytic materials are studied. In addition, the effectiveness of combining GI and LEZ is also investigated. For real scenarios, emission reductions corresponding to a LEZ is difficult to estimate depending on the traffic restrictions. For this reason, in this study, a range of concentration reductions within the LEZ and increases of concentration in the streets surrounding the LEZ are considered. In this way, a range of concentration reductions at pedestrian level induced by LEZ is shown. In addition, this paper does not aim to model specific species of vegetation (trees, hedgerows, etc.…) and for this reason, several values of typical deposition velocity are also considered. Deposition velocity depends on type of air pollutant and characteristics and conditions of plant species. In this way, the contribution of deposition and aerodynamic effects of GI on air quality is investigated for several cases. Typical values of LAD are also studied. More details can be found in Santiago et al. (2022d). For an appropriate plant selection, the cost-benefits of each plant species and the suitability of each one to the environmental conditions of the intended planting location should be taken into account (Barwise and Kumar, 2020).

Main conclusions obtained can be summarized as follows:

- Photocatalytic materials provide small concentration reductions (< 4 %) in this urban environment, and consequently, the use of these materials seems to be a non-effective measure.
- LEZ is found to be the most effective individual measure investigated. Concentration reductions depend on the intensity of LEZ restrictions and traffic diversion around LEZ. Concentration reductions are spatially heterogeneous and, in the cases with strong traffic diversion, concentrations increase with respect to the base scenario in some areas. This issue indicates the importance of an appropriate design of LEZ to be effective for improving air quality. On one hand, traffic emissions should be reduced as much as possible within the LEZ, but on the other, traffic restrictions should be accompanied by measures aimed at preventing the traffic diversion, which could increase the air pollutant emission around LEZ.
- The effectiveness of a GI strongly depends on the configuration of its vegetation elements and it is very heterogeneous at pedestrian level. Current results, which agree with previous studies (Abhijith et al., 2017; Buccolieri et al., 2018a), show that GI alone cannot be considered as a general air quality mitigation measure within streets. In general, the aerodynamics effects of street trees tend to increase air pollutant concentrations at pedestrian level, in particular for streets with low aspect ratio like the streets of this study with H/W = 1. However, the present study shows that appropriate configurations of trees and hedgerow in the streets, and including air pollutant deposition, can provide significant improvements on air pollutant concentrations at pedestrian level. Uncertainty about the effect of the GI can rise from uncertainties about the real deposition velocities. Additionally, these results are for trees being clearly lower than the building. Surely, further studies considering other width/height ratio street canyon and different height of trees must be done in the future to elucidate whether these conclusions could be generalized. In

addition, alternative configurations of GI considering the variation of other parameters such as separation between trees, shapes of crown or LAD could be considered in future studies to optimize the impact of GIs.

- The effectiveness of GI in reducing pedestrian level concentrations is enhanced by combining GI and LEZ. The effectiveness strongly depends on GI layout including the characteristics of vegetation elements, the intensity of emission reduction and the traffic diversion in streets that surround LEZ. For more restricted LEZ avoiding traffic diversion, concentration reductions are found at pedestrian level, even for most unfavorable GI configurations (when GI is implanted alone). This point is important as, in addition to the effects of vegetation on urban air quality, the set of benefits on city dweller is much broader (microclimate regulation, reducing noise, enhancing biodiversity, making urban environment more pleasant, psychological values, etc.…). Therefore, benefits in different aspects are provided by urban vegetation and their design should be addressed as a trade-off of services and disservices provided. In this way, current results present how the emission reductions through a LEZ can prevent the possible negative effects of any GI configuration due to the reduction of street ventilation on air quality, and any GI can be implemented for providing other ecosystem services avoiding those problems implemented a LEZ at the same time.

Current results can be extrapolated to scenarios with similar building morphologies (high-rise buildings separated by avenues with an aspect ratio of one and a planar building packing density of 0.25). For more complex urban areas, wind flow and air pollutant dispersion are also more complex and particular studies should be addressed in future investigations. Considering the discrepancies in the literature (Buccolieri et al., 2018a, 2018b), the values of deposition velocity for each studied pollutant could range from 0.01 to 0.05 m s-1.

The limitations of this study must be considered for generalizing the present results for urban planning and policy decisions. The first limitation is the assumption that pollutants are considered as non-reactive pollutants emitted by traffic. This assumption is reasonable for the simulation domain considered, but they must be taken into account for successful policy planning. The second limitation is the correspondence between deposition velocity, plant species, and pollutants. The discrepancies between deposition velocities found in the literature (Buccolieri et al., 2018a, 2018b) make it difficult to determine this correspondence and consequently, the use of the simulation results by policymakers. In the present study, three different deposition velocities (0, 0.01, and 0.05 m s-1) within the range of published values are simulated to provide results within a realistic range of conditions. For the use of the present study results by policymakers, they must estimate the most appropriate deposition velocity for the pollutant and the species that is intended to be implemented. Specific studies on this should be carried out previously. This paper can help to take one more step towards the understanding of the effects of these measures to improve air quality. For urban planning and policy decisions, the main conclusions of this paper is that the designs of GI and LEZ are crucial for improving air quality at pedestrian level and the combination of both measures is recommended. To improve air quality, GI should be designed to avoid the reduction of street ventilation. However, the implementation of GI within a LEZ prevents the possible negative effects on air quality of the reduction of street ventilation if the intensity of traffic restrictions is large enough, and GI can be implemented for providing other ecosystem services (e.g., microclimate regulation).

## CRediT authorship contribution statement

**J.L. Santiago:** Writing – original draft, Methodology, Formal analysis, Conceptualization. **E. Rivas:** Writing – review & editing, Validation, Software, Methodology. **B. Sanchez:** Writing – review & editing, Validation, Methodology, Conceptualization. **R. Buccolieri:** Writing – review & editing, Methodology. **M.G. Vivanco:** Writing – review & editing, Methodology, Conceptualization. **A. Martilli:** Writing – review & editing, Methodology, Conceptualization. **F. Martín:** Writing – review & editing, Methodology, Conceptualization.

## Declaration of competing interest

The authors declare that they have no known competing financial interests or personal relationships that could have appeared to influence the work reported in this paper.

## Data availability

Data will be made available on request.

## Acknowledgements

This study is part of the RETOS-AIRE project (Grant: RTI2018-099138-B-I00) funded by MCIN/AEI/10.13039/501100011033 and by ERDF A way of making Europe. This study was also supported by AIRTEC-CM (S2018/EMT-4329) research project funded by Regional Government of Madrid. This work was partially supported by the computing facilities of Extremadura Research Centre for Advanced Technologies (CETA-CIEMAT), funded by the European Regional Development Fund (ERDF). CETA-CIEMAT belongs to CIEMAT and the Government of Spain.

## Appendix A

Maps of $C_{norm}$ at 3 m-height for all LEZ + GI scenarios for 0° and 45° wind directions (with the exception of *LEZ_0.2 + VEG_TreesMedian* and *LEZ_0.8 + VEG_TreesMedian* for 0° wind direction, that are already presented in Section 3.4) are shown in this Appendix

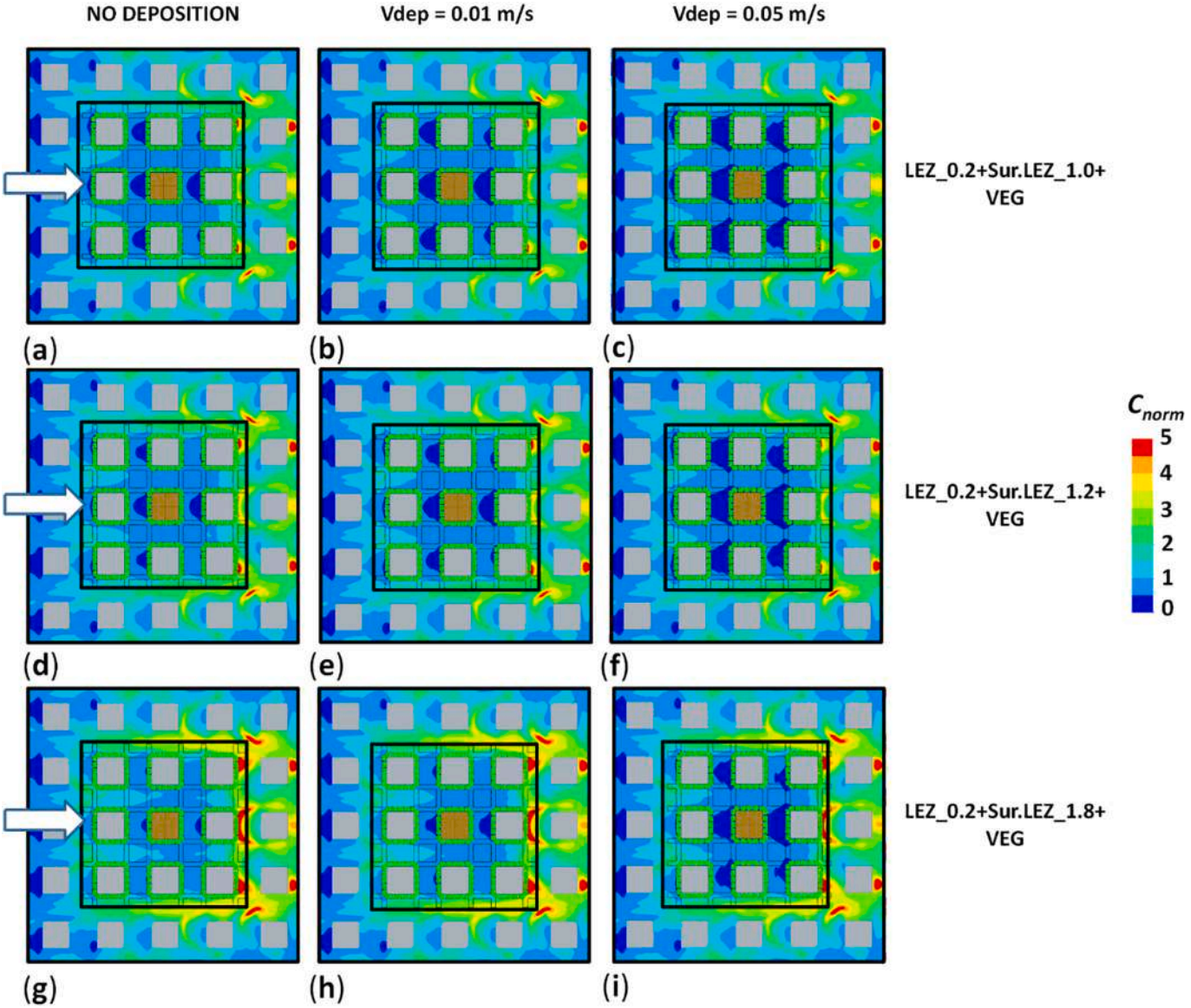


**Fig. A1.** *LEZ_0.2* scenarios with GI (VEG): maps of $C_{norm}$ at 3 m-height. (a) *LEZ_0.2 + SurroundLEZ_1.0 + VEG* scenario without deposition for 0° wind direction. (b) Same as (a) but with $V_{dep} = 0.01$ m s$^{-1}$. (c) Same as (a) but with $V_{dep} = 0.05$ m s$^{-1}$. (d) *LEZ_0.2 + SurroundLEZ_1.2 + VEG* scenario without deposition for 0° wind direction. (e) Same as (d) but with $V_{dep} = 0.01$ m s$^{-1}$. (f) Same as (d) but with $V_{dep} = 0.05$ m s$^{-1}$. (g) *LEZ_0.2 + SurroundLEZ_1.8 + VEG* scenario without deposition for 0° wind direction. (h) Same as (g) but with $V_{dep} = 0.01$ m s$^{-1}$. (i) Same as (g) but with $V_{dep} = 0.05$ m s$^{-1}$.

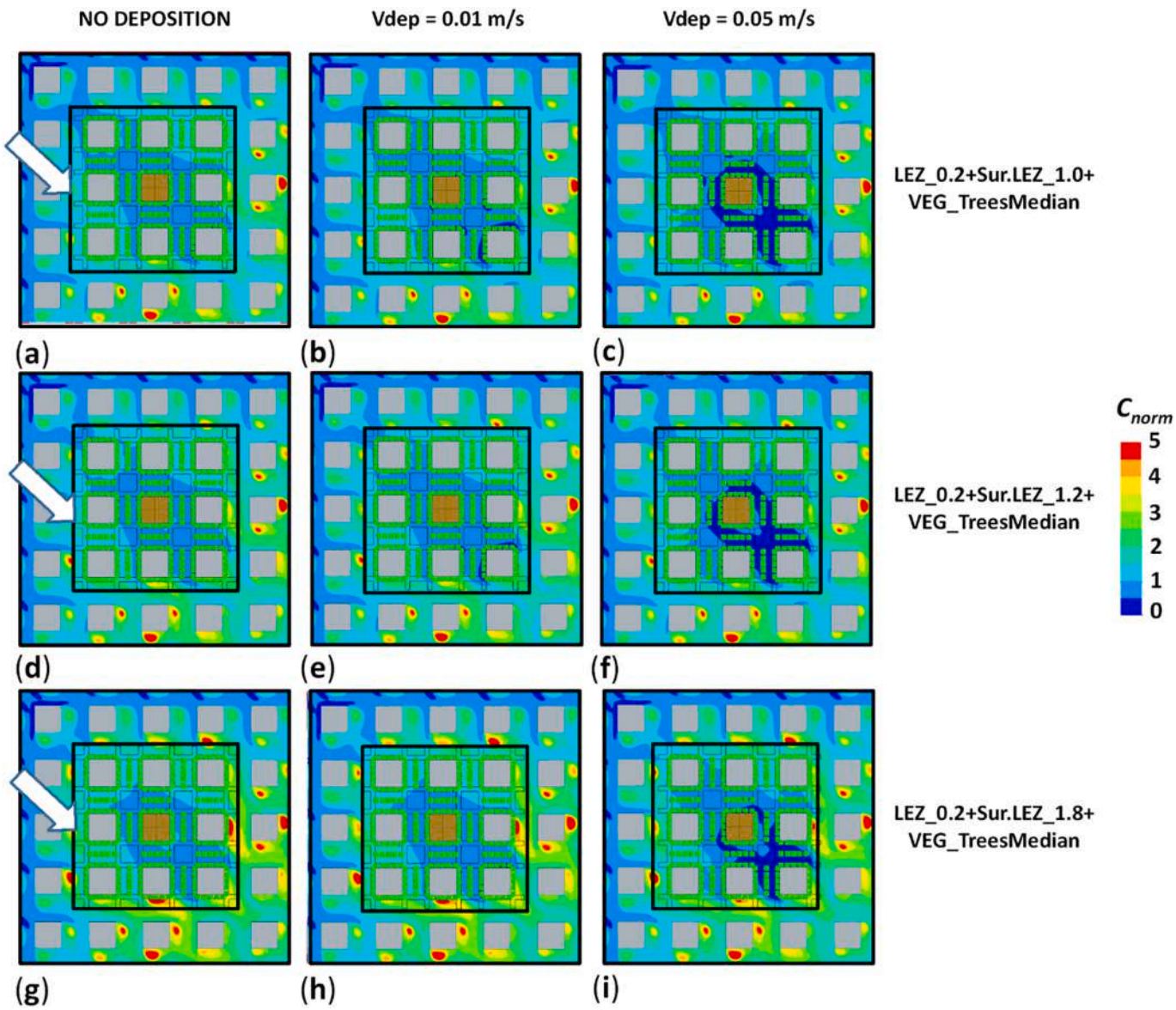


**Fig. A2.** *LEZ_0.2* scenarios with GI (VEG_TreesMedian): maps of $C_{norm}$ at 3 m-height. (a) *LEZ_0.2 + SurroundLEZ_1.0 + VEG_TreesMedian* scenario without deposition for 45° wind direction. (b) Same as (a) but with $V_{dep} = 0.01$ m s$^{-1}$. (c) Same as (a) but with $V_{dep} = 0.05$ m s$^{-1}$. (d) *LEZ_0.2 + SurroundLEZ_1.2 + VEG_TreesMedian* scenario without deposition for 45° wind direction. (e) Same as (d) but with $V_{dep} = 0.01$ m s$^{-1}$. (f) Same as (d) but with $V_{dep} = 0.05$ m s$^{-1}$. (g) *LEZ_0.2 + SurroundLEZ_1.8 + VEG_TreesMedian* scenario without deposition for 45° wind direction. (h) Same as (g) but with $V_{dep} = 0.01$ m s$^{-1}$. (i) Same as (g) but with $V_{dep} = 0.05$ m s$^{-1}$.

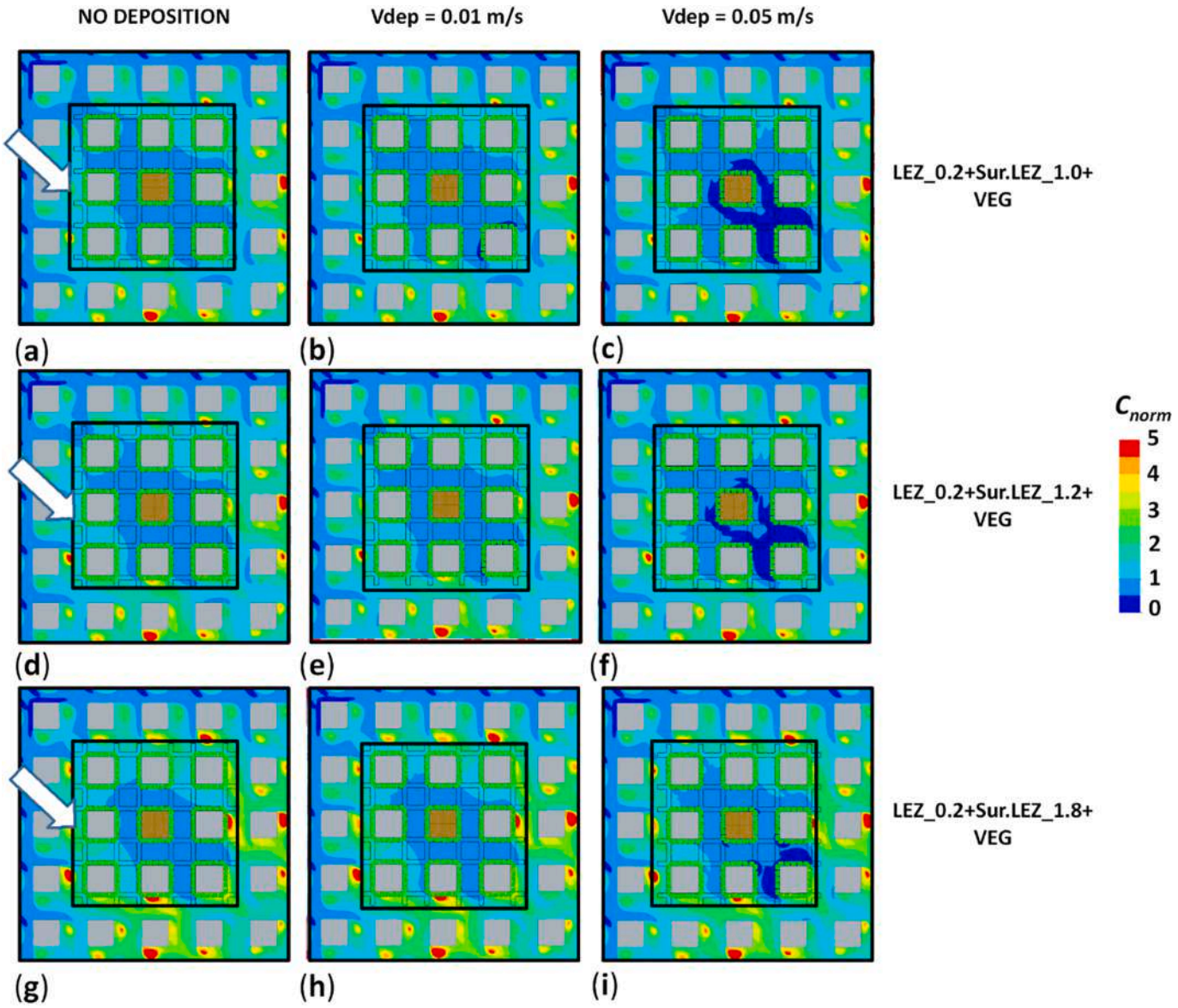


**Fig. A3.** *LEZ_0.2* scenarios with GI (VEG): maps of $C_{norm}$ at 3 m-height. (a) *LEZ_0.2* + *SurroundLEZ_1.0* + *VEG* scenario without deposition for 45° wind direction. (b) Same as (a) but with $V_{dep} = 0.01$ m s$^{-1}$. (c) Same as (a) but with $V_{dep} = 0.05$ m s$^{-1}$. (d) *LEZ_0.2* + *SurroundLEZ_1.2* + *VEG* scenario without deposition for 45° wind direction. (e) Same as (d) but with $V_{dep} = 0.01$ m s$^{-1}$. (f) Same as (d) but with $V_{dep} = 0.05$ m s$^{-1}$. (g) *LEZ_0.2* + *SurroundLEZ_1.8* + *VEG* scenario without deposition for 45° wind direction. (h) Same as (g) but with $V_{dep} = 0.01$ m s$^{-1}$. (i) Same as (g) but with $V_{dep} = 0.05$ m s$^{-1}$.

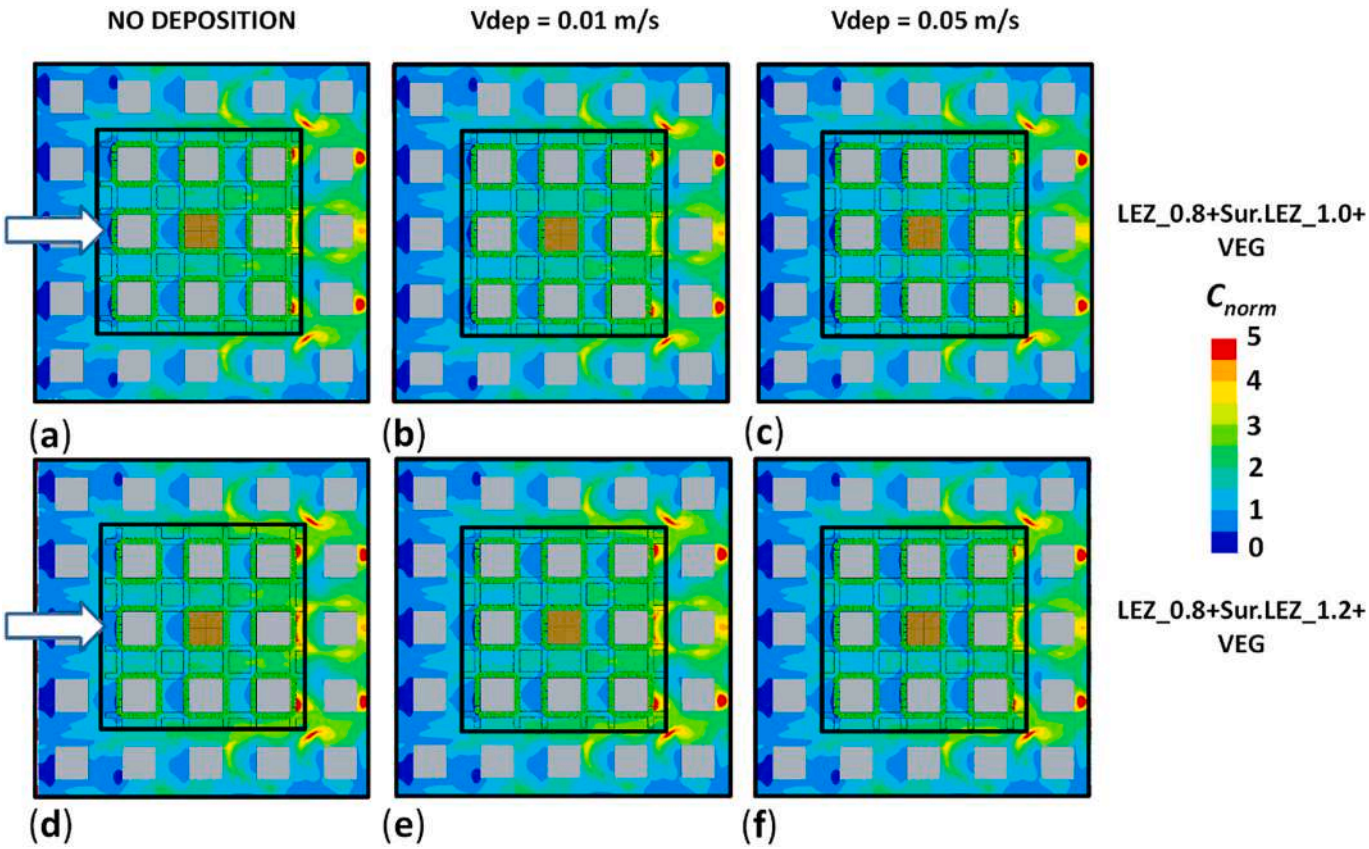


**Fig. A4.** *LEZ_0.8* scenarios with GI (VEG): maps of $C_{norm}$ at 3 m-height. (a) *LEZ_0.8* + *SurroundLEZ_1.0* + *VEG* scenario without deposition for 0° wind direction. (b) Same as (a) but with $V_{dep} = 0.01$ m s$^{-1}$. (c) Same as (a) but with $V_{dep} = 0.05$ m s$^{-1}$. (d) *LEZ_0.8* + *SurroundLEZ_1.2* + *VEG* scenario without deposition for 0° wind direction. (e) Same as (d) but with $V_{dep} = 0.01$ m s$^{-1}$. (f) Same as (d) but with $V_{dep} = 0.05$ m s$^{-1}$.

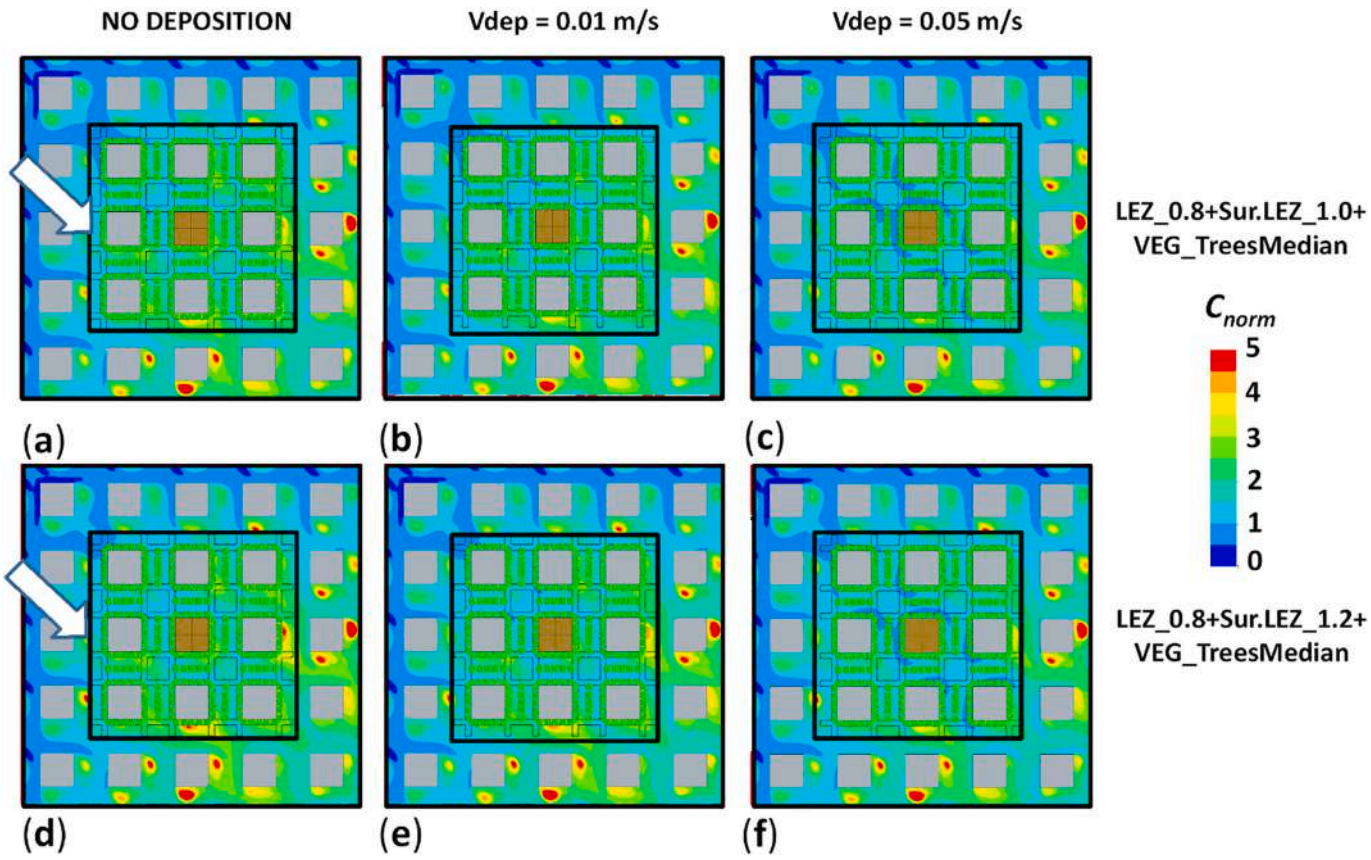


**Fig. A5.** *LEZ_0.8* scenarios with GI (VEG_TreesMedian): maps of $C_{norm}$ at 3 m-height. (a) *LEZ_0.8 + SurroundLEZ_1.0 + VEG_TreesMedian* scenario without deposition for 45° wind direction. (b) Same as (a) but with $V_{dep} = 0.01$ m s$^{-1}$. (c) Same as (a) but with $V_{dep} = 0.05$ m s$^{-1}$. (d) *LEZ_0.8 + SurroundLEZ_1.2 + VEG_TreesMedian* scenario without deposition for 45° wind direction. (e) Same as (d) but with $V_{dep} = 0.01$ m s$^{-1}$. (f) Same as (d) but with $V_{dep} = 0.05$ m s$^{-1}$.

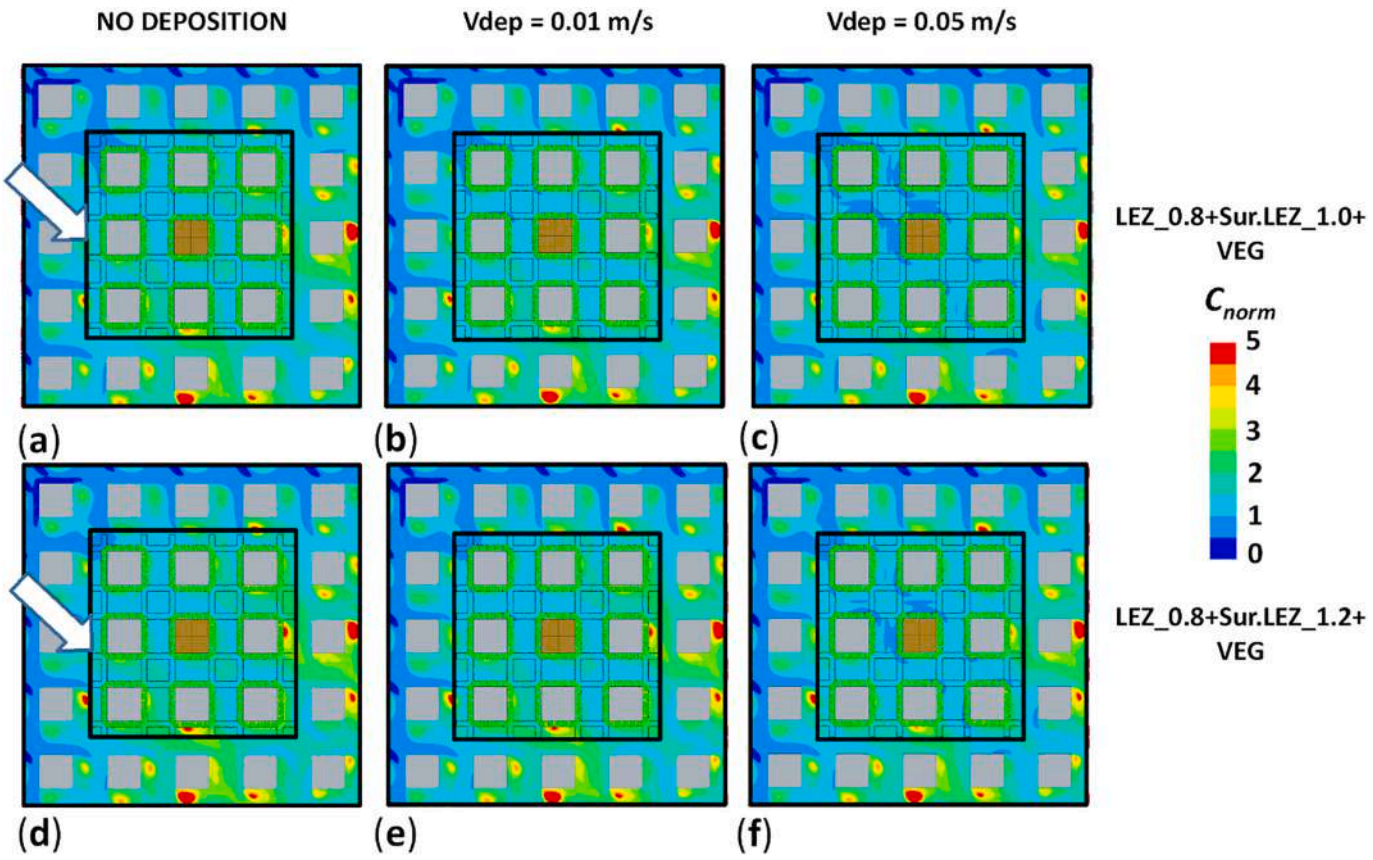


**Fig. A6.** *LEZ_0.8* scenarios with GI (VEG): maps of $C_{norm}$ at 3 m-height. (a) *LEZ_0.8 + SurroundLEZ_1.0 + VEG* scenario without deposition for 45° wind direction. (b) Same as (a) but with $V_{dep} = 0.01$ m s$^{-1}$. (c) Same as (a) but with $V_{dep} = 0.05$ m s$^{-1}$. (d) *LEZ_0.8 + SurroundLEZ_1.2 + VEG* scenario without deposition for 45° wind direction. (e) Same as (d) but with $V_{dep} = 0.01$ m s$^{-1}$. (f) Same as (d) but with $V_{dep} = 0.05$ m s$^{-1}$.

## Appendix B

Tables with the variations of the spatially-averaged concentrations in comparison with BASE scenarios over different areas (*Building, Sidewalks, Neighborhood, Surrounding and Neighborhood + Surrounding*) at pedestrian level for both wind directions (in %)

**Table B1**
LEZ scenarios: variations of the spatially-averaged concentrations in comparison with BASE scenarios over different areas (*Building, Sidewalks, Neighborhood, Surrounding and Neighborhood + Surrounding*) at pedestrian level for 0° wind direction (in %). Green for concentration reductions higher than 15 %; Light green for concentration reductions between 5 % and 15 %; White for variation of concentrations between 5 % and -5 %; Light red for increases of concentrations between 5 % and 15 %; Red for increases of concentrations higher than 15 %.

| | *Building* | *Sidewalks* | *Neighborhood* | *Surrounding* | *Neighborhood + Surrounding* |
|---|---|---|---|---|---|
| ***LEZ_0.2 +SurroundLEZ_1.0*** | -59% | -39% | -39% | -4% | -17% |
| ***LEZ_0.2 +SurroundLEZ_1.2*** | -57% | -33% | -33% | 1% | -12% |
| ***LEZ_0.2 +SurroundLEZ_1.8*** | -52% | -14% | -14% | 15% | 4% |
| ***LEZ_0.8 +SurroundLEZ_1.0*** | -15% | -10% | -10% | -1% | -4% |
| ***LEZ_0.8 +SurroundLEZ_1.2*** | -13% | -4% | -3% | 4% | 1% |

**Table B2**
LEZ scenarios: variations of the spatially-averaged concentrations in comparison with BASE scenarios over different areas (*Building, Sidewalks, Neighborhood, Surrounding and Neighborhood + Surrounding*) at pedestrian level for 45° wind direction (in %). Green for concentration reductions higher than 15 %; Light green for concentration reductions between 5 % and 15 %; White for variation of concentrations between 5 % and − 5 %; Light red for increases of concentrations between 5 % and 15 %; Red for increases of concentrations higher than 15 %.

| | *Building* | *Sidewalks* | *Neighborhood* | *Surrounding* | *Neighborhood + Surrounding* |
|---|---|---|---|---|---|
| ***LEZ_0.2 +SurroundLEZ_1.0*** | -61% | -41% | -41% | -7% | -21% |
| ***LEZ_0.2 +SurroundLEZ_1.2*** | -59% | -36% | -36% | -3% | -16% |
| ***LEZ_0.2 +SurroundLEZ_1.8*** | -54% | -19% | -19% | 11% | -1% |
| ***LEZ_0.8 +SurroundLEZ_1.0*** | -15% | -10% | -10% | -2% | -5% |
| ***LEZ_0.8 +SurroundLEZ_1.2*** | -13% | -5% | -5% | 3% | 0% |

**Table B3**
GI scenarios: variations of the spatially-averaged concentrations in comparison with BASE scenarios over different areas (*Building*, *Sidewalks* and *Neighborhood*) at pedestrian level for 0° wind direction (in %). Green for concentration reductions higher than 15 %; Light green for concentration reductions between 5 % and 15 %; White for variation of concentrations between 5 % and -5 %; Light red for increases of concentrations between 5 % and 15 %; Red for increases of concentrations higher than 15 %.

| | *Building* | *Sidewalks* | *Neighborhood* |
|---|---|---|---|
| ***VEG (NO Deposition)*** | 6% | 8% | 7% |
| ***VEG (Vdep = 0.01 m $s^{-1}$)*** | -3% | 1% | 1% |
| ***VEG (Vdep = 0.05 m $s^{-1}$)*** | -26% | -15% | -12% |
| ***VEG_TreesMedian (NO Deposition)*** | 36% | 23% | 25% |
| ***VEG_TreesMedian (Vdep = 0.01 m $s^{-1}$)*** | 18% | 13% | 16% |
| ***VEG_TreesMedian (Vdep = 0.05 m $s^{-1}$)*** | -20% | -9% | -5% |

**Table B4**
GI scenarios: variations of the spatially-averaged concentrations in comparison with BASE scenarios over different areas (*Building*, *Sidewalks* and *Neighborhood*) at pedestrian level for 45° wind direction (in %). Green for concentration reductions higher than 15 %; Light green for concentration reductions between 5 % and 15 %; White for variation of concentrations between 5 % and -5 %; Light red for increases of concentrations between 5 % and 15 %; Red for increases of concentrations higher than 15 %.

| | *Building* | *Sidewalks* | *Neighborhood* |
|---|---|---|---|
| ***VEG (NO Deposition)*** | -4% | 3% | -4% |
| ***VEG (Vdep = 0.01 m $s^{-1}$)*** | -11% | -2% | -9% |
| ***VEG (Vdep = 0.05 m $s^{-1}$)*** | -27% | -16% | -21% |
| ***VEG_TreesMedian (NO Deposition)*** | 6% | 12% | 4% |
| ***VEG_TreesMedian (Vdep = 0.01 m $s^{-1}$)*** | -3% | 5% | -2% |
| ***VEG_TreesMedian (Vdep = 0.05 m $s^{-1}$)*** | -24% | -13% | -18% |

**Table B5**
LEZ_0.2 scenarios with GI (*VEG* and *VEG_TreesMedian* scenarios): variations in comparison with BASE scenarios of the spatially-averaged concentrations over different areas (*Building*, *Sidewalks*, *Neighborhood, Surrounding* and *Neighborhood + Surrounding*) for 0° wind direction (in %). Green for concentration reductions higher than 15 %; Light green for concentration reductions between 5 % and 15 %; White for variation of concentrations between 5 % and − 5 %; Light red for increases of concentrations between 5 % and 15 %; Red for increases of concentrations higher than 15 %.

| | *Building* | *Sidewalks* | *Neighborhood* | *Surrounding* | *Neighborhood + Surrounding* |
|---|---|---|---|---|---|
| *LEZ_0.2 +SurroundLEZ_1.0 + VEG (NO Deposition)* | -57% | -35% | -35% | -4% | -16% |
| *LEZ_0.2 +SurroundLEZ_1.0 + VEG (Vdep = 0.01 m s$^{-1}$)* | -62% | -38% | -38% | -5% | -18% |
| *LEZ_0.2 +SurroundLEZ_1.0 + VEG (Vdep=0.05 m s$^{-1}$)* | -73% | -48% | -46% | -6% | -22% |
| *LEZ_0.2 +SurroundLEZ_1.0 + VEG_TreesMedian (NO Deposition)* | -52% | -29% | -28% | -4% | -13% |
| *LEZ_0.2 +SurroundLEZ_1.0 + VEG_TreesMedian (Vdep = 0.01 m s$^{-1}$)* | -60% | -34% | -33% | -5% | -16% |
| *LEZ_0.2 +SurroundLEZ_1.0 + VEG_TreesMedian (Vdep = 0.05 m s$^{-1}$)* | -75% | -46% | -44% | -6% | -21% |
| *LEZ_0.2 +SurroundLEZ_1.2 + VEG (NO Deposition)* | -56% | -28% | -28% | 0% | -11% |
| *LEZ_0.2 +SurroundLEZ_1.2 + VEG (Vdep = 0.01 m s$^{-1}$)* | -60% | -32% | -31% | 0% | -12% |
| *LEZ_0.2 +SurroundLEZ_1.2 + VEG (Vdep=0.05 m s$^{-1}$)* | -71% | -42% | -40% | -2% | -17% |
| *LEZ_0.2 +SurroundLEZ_1.2 + VEG_TreesMedian (NO Deposition)* | -50% | -21% | -21% | 0% | -8% |
| *LEZ_0.2 +SurroundLEZ_1.2 + VEG_TreesMedian (Vdep = 0.01 m s$^{-1}$)* | -58% | -27% | -26% | 0% | -10% |
| *LEZ_0.2 +SurroundLEZ_1.2 + VEG_TreesMedian (Vdep = 0.05 m s$^{-1}$)* | -74% | -40% | -38% | -2% | -16% |
| *LEZ_0.2 +SurroundLEZ_1.8 + VEG (NO Deposition)* | -50% | -7% | -8% | 14% | 5% |
| *LEZ_0.2 +SurroundLEZ_1.8 + VEG (Vdep = 0.01 m s$^{-1}$)* | -55% | -12% | -12% | 13% | 3% |
| *LEZ_0.2 +SurroundLEZ_1.8 + VEG (Vdep=0.05 m s$^{-1}$)* | -68% | -25% | -22% | 11% | -2% |
| *LEZ_0.2 +SurroundLEZ_1.8 + VEG_TreesMedian (NO Deposition)* | -45% | 1% | 1% | 14% | 9% |
| *LEZ_0.2 +SurroundLEZ_1.8 + VEG_TreesMedian (Vdep = 0.01 m s$^{-1}$)* | -54% | -6% | -5% | 13% | 6% |
| *LEZ_0.2 +SurroundLEZ_1.8 + VEG_TreesMedian (Vdep = 0.05 m s$^{-1}$)* | -72% | -22% | -19% | 10% | -1% |

**Table B6**
LEZ_0.2 scenarios with GI (*VEG* and *VEG_TreesMedian* scenarios): variations in comparison with BASE scenarios of the spatially-averaged concentrations over different areas (*Building*, *Sidewalks*, *Neighborhood, Surrounding* and *Neighborhood + Surrounding*) for 45° wind direction (in %). Green for concentration reductions higher than 15 %; Light green for concentration reductions between 5 % and 15 %; White for variation of concentrations between 5 % and -5 %; Light red for increases of concentrations between 5 % and 15 %; Red for increases of concentrations higher than 15 %.

| | *Building* | *Sidewalks* | *Neighborhood* | *Surrounding* | *Neighborhood + Surrounding* |
|---|---|---|---|---|---|
| *LEZ_0.2 +SurroundLEZ_1.0 + VEG (NO Deposition)* | -65% | -40% | -43% | -4% | -20% |
| *LEZ_0.2 +SurroundLEZ_1.0 + VEG (Vdep = 0.01 m s$^{-1}$)* | -68% | -43% | -46% | -5% | -21% |
| *LEZ_0.2 +SurroundLEZ_1.0 + VEG (Vdep=0.05 m s$^{-1}$)* | -75% | -51% | -53% | -6% | -25% |
| *LEZ_0.2 +SurroundLEZ_1.0 + VEG_TreesMedian (NO Deposition)* | -63% | -37% | -40% | -1% | -17% |
| *LEZ_0.2 +SurroundLEZ_1.0 + VEG_TreesMedian (Vdep = 0.01 m s$^{-1}$)* | -67% | -41% | -44% | -2% | -19% |
| *LEZ_0.2 +SurroundLEZ_1.0 + VEG_TreesMedian (Vdep = 0.05 m s$^{-1}$)* | -76% | -51% | -53% | -4% | -24% |
| *LEZ_0.2 +SurroundLEZ_1.2 + VEG (NO Deposition)* | -63% | -34% | -38% | 1% | -15% |
| *LEZ_0.2 +SurroundLEZ_1.2 + VEG (Vdep = 0.01 m s$^{-1}$)* | -66% | -38% | -41% | 0% | -16% |
| *LEZ_0.2 +SurroundLEZ_1.2 + VEG (Vdep=0.05 m s$^{-1}$)* | -74% | -46% | -48% | -2% | -21% |
| *LEZ_0.2 +SurroundLEZ_1.2 + VEG_TreesMedian (NO Deposition)* | -61% | -31% | -35% | 5% | -11% |
| *LEZ_0.2 +SurroundLEZ_1.2 + VEG_TreesMedian (Vdep = 0.01 m s$^{-1}$)* | -66% | -36% | -39% | 4% | -14% |
| *LEZ_0.2 +SurroundLEZ_1.2 + VEG_TreesMedian (Vdep = 0.05 m s$^{-1}$)* | -75% | -47% | -48% | 1% | -19% |
| *LEZ_0.2 +SurroundLEZ_1.8 + VEG (NO Deposition)* | -58% | -17% | -21% | 16% | 1% |
| *LEZ_0.2 +SurroundLEZ_1.8 + VEG (Vdep = 0.01 m s$^{-1}$)* | -62% | -21% | -25% | 15% | -1% |
| *LEZ_0.2 +SurroundLEZ_1.8 + VEG (Vdep=0.05 m s$^{-1}$)* | -71% | -32% | -34% | 12% | -6% |
| *LEZ_0.2 +SurroundLEZ_1.8 + VEG_TreesMedian (NO Deposition)* | -57% | -14% | -17% | 20% | 5% |
| *LEZ_0.2 +SurroundLEZ_1.8 + VEG_TreesMedian (Vdep = 0.01 m s$^{-1}$)* | -62% | -19% | -22% | 19% | 2% |
| *LEZ_0.2 +SurroundLEZ_1.8 + VEG_TreesMedian (Vdep = 0.05 m s$^{-1}$)* | -73% | -32% | -33% | 16% | -4% |

**Table B7**
LEZ_0.8 scenarios with GI (*VEG* and *VEG_TreesMedian* scenarios): variations in comparison with BASE scenarios of the spatially-averaged concentrations over different areas (*Building*, *Sidewalks*, *Neighborhood, Surrounding* and *Neighborhood + Surrounding*) for 0° wind direction (in %). Green for concentration reductions higher than 15 %; Light green for concentration reductions between 5 % and 15 %; White for variation of concentrations between 5 % and -5 %; Light red for increases of concentrations between 5 % and 15 %; Red for increases of concentrations higher than 15 %.

| | ***Building*** | ***Sidewalks*** | ***Neighborhood*** | ***Surrounding*** | ***Neighborhood + Surrounding*** |
|---|---|---|---|---|---|
| ***LEZ_0.8 +SurroundLEZ_1.0 + VEG (NO Deposition)*** | -10% | -3% | -4% | -1% | -2% |
| ***LEZ_0.8 +SurroundLEZ_1.0 + VEG (Vdep = 0.01 m $s^{-1}$)*** | -18% | -9% | -9% | -2% | -5% |
| ***LEZ_0.8 +SurroundLEZ_1.0 + VEG (Vdep=0.05 m $s^{-1}$)*** | -38% | -23% | -21% | -4% | -11% |
| ***LEZ_0.8 +SurroundLEZ_1.0 + VEG_TreesMedian (NO Deposition)*** | 14% | 10% | 12% | -2% | 4% |
| ***LEZ_0.8 +SurroundLEZ_1.0 + VEG_TreesMedian (Vdep = 0.01 m $s^{-1}$)*** | -1% | 1% | 3% | -2% | 0% |
| ***LEZ_0.8 +SurroundLEZ_1.0*** | -34% | -19% | -15% | -5% | -9% |
| ***+ VEG_TreesMedian (Vdep = 0.05 m $s^{-1}$)*** | | | | | |
| ***LEZ_0.8 +SurroundLEZ_1.2 + VEG (NO Deposition)*** | -8% | 4% | 3% | 3% | 3% |
| ***LEZ_0.8 +SurroundLEZ_1.2 + VEG (Vdep = 0.01 m $s^{-1}$)*** | -16% | -2% | -2% | 2% | 1% |
| ***LEZ_0.8 +SurroundLEZ_1.2 + VEG (Vdep=0.05 m $s^{-1}$)*** | -37% | -18% | -15% | 0% | -6% |
| ***LEZ_0.8 +SurroundLEZ_1.2 + VEG_TreesMedian (NO Deposition)*** | 16% | 17% | 19% | 3% | 9% |
| ***LEZ_0.8 +SurroundLEZ_1.2 + VEG_TreesMedian (Vdep = 0.01 m $s^{-1}$)*** | 0% | 8% | 10% | 2% | 5% |
| ***LEZ_0.8 +SurroundLEZ_1.2 + VEG_TreesMedian (Vdep = 0.05 m $s^{-1}$)*** | -33% | -13% | -8% | -1% | -4% |

**Table B8**
LEZ_0.8 scenarios with GI (*VEG* and *VEG_TreesMedian* scenarios): variations in comparison with BASE scenarios of the spatially-averaged concentrations over different areas (*Building*, *Sidewalks*, *Neighborhood, Surrounding* and *Neighborhood + Surrounding*) for 45° wind direction (in %). Green for concentration reductions higher than 15 %; Light green for concentration reductions between 5 % and 15 %; White for variation of concentrations between 5 % and -5 %; Light red for increases of concentrations between 5 % and 15 %; Red for increases of concentrations higher than 15 %.

| | *Building* | *Sidewalks* | *Neighborhood* | *Surrounding* | *Neighborhood + Surrounding* |
|---|---|---|---|---|---|
| ***LEZ_0.8 +SurroundLEZ_1.0 + VEG (NO Deposition)*** | -19% | -8% | -14% | 1% | -5% |
| ***LEZ_0.8 +SurroundLEZ_1.0 + VEG (Vdep = 0.01 m $s^{-1}$)*** | -25% | -13% | -18% | 0% | -7% |
| ***LEZ_0.8 +SurroundLEZ_1.0 + VEG (Vdep=0.05 m $s^{-1}$)*** | -39% | -25% | -29% | -3% | -13% |
| ***LEZ_0.8 +SurroundLEZ_1.0 + VEG_TreesMedian (NO Deposition)*** | -12% | 0% | -7% | 4% | 0% |
| ***LEZ_0.8 +SurroundLEZ_1.0 + VEG_TreesMedian (Vdep = 0.01 m $s^{-1}$)*** | -19% | -7% | -13% | 3% | -4% |
| ***LEZ_0.8 +SurroundLEZ_1.0 + VEG_TreesMedian (Vdep = 0.05 m $s^{-1}$)*** | -37% | -23% | -27% | -1% | -11% |
| ***LEZ_0.8 +SurroundLEZ_1.2 + VEG (NO Deposition)*** | -18% | -2% | -9% | 6% | 0% |
| ***LEZ_0.8 +SurroundLEZ_1.2 + VEG (Vdep = 0.01 m $s^{-1}$)*** | -23% | -7% | -13% | 5% | -2% |
| ***LEZ_0.8 +SurroundLEZ_1.2 + VEG (Vdep=0.05 m $s^{-1}$)*** | -38% | -20% | -24% | 2% | -9% |
| ***LEZ_0.8 +SurroundLEZ_1.2 + VEG_TreesMedian (NO Deposition)*** | -10% | 6% | -1% | 9% | 5% |
| ***LEZ_0.8 +SurroundLEZ_1.2 + VEG_TreesMedian (Vdep = 0.01 m $s^{-1}$)*** | -18% | -1% | -7% | 8% | 2% |
| ***LEZ_0.8 +SurroundLEZ_1.2 + VEG_TreesMedian (Vdep = 0.05 m $s^{-1}$)*** | -36% | -18% | -22% | 4% | -6% |

## References


Abhijith, K.V., Kumar, P., Gallagher, J., McNabola, A., Baldauf, R., Pilla, F., Broderick, B., Di Sabatino, S., Pulvirenti, B., 2017. Air pollution abatement performances of green infrastructure in open road and built-up street canyon environments-a review. Atmos. Environ. 162, 71–86. https://doi.org/10.1016/j.atmosenv.2017.05.014.

Amorim, J.H., Rodrigues, V., Tavares, R., Valente, J., Borrego, C., 2013. CFD modelling of the aerodynamic effect of trees on urban air pollution dispersion. Sci. Total Environ. 461, 541–551. https://doi.org/10.1016/j.scitotenv.2013.05.031.

Angelidis, D., Assimakopoulos, V., Bergeles, G., 2012. 3D flow and pollutant dispersion simulation in organized cubic structures. In: Progress in Hybrid RANS-LES Modelling. Springer, Berlin, Heidelberg, pp. 503–513.

Barwise, Y., Kumar, P., 2020. Designing vegetation barriers for urban air pollution abatement: a practical review for appropriate plant species selection. npj Clim. Atmos. Sci. 3 (1), 1–19. https://doi.org/10.1038/s41612-020-0115-3.

Boogaard, H., Janssen, N.A., Fischer, P.H., Kos, G.P., Weijers, E.P., Cassee, F.R., van der Zee, S.C., de Hartog, J.J., Meliefste, K., Wang, M., Brunekreef, B., Hoek, G., 2012. Impact of low emission zones and local traffic policies on ambient air pollution concentrations. Sci. Total Environ. 435, 132–140. https://doi.org/10.1016/j.scitotenv.2012.06.089.

Borge, R., Narros, A., Artíñano, B., Yagüe, C., Gómez-Moreno, F.J., de la Paz, D., Roman-Cascon, C., Díaz, E., Maqueda, G., Sastre, M., Quaassdorff, C., Dimitroulopoulou, C., Vardoulakis, S., 2016. Assessment of microscale spatio-temporal variation of air pollution at an urban hotspot in Madrid (Spain) through an extensive field campaign. Atmos. Environ. 2016 (140), 432–445. https://doi.org/10.1016/j.atmosenv.2016.06.020.

Brown, M.J., Lawson, R.E., DeCroix, D.S., Lee, R.L., 2001. Comparison of Centerline Velocity Measurements Obtained around 2D and 3D Buildings Arrays in a Wind Tunnel, Report LA-UR-01–4138. Los Alamos National Laboratory, Los Alamos, p. 7.

Buccolieri, R., Salim, S.M., Leo, L.S., Di Sabatino, S., Chan, A., Ielpo, P., Gromke, C., 2011. Analysis of local scale tree–atmosphere interaction on pollutant concentration

in idealized street canyons and application to a real urban junction. Atmos. Environ. 45, 1702–1713. https://doi.org/10.1016/j.atmosenv.2010.12.058.
Buccolieri, R., Jeanjean, A.P.R., Gatto, E., Leigh, R.J., 2018a. The impact of trees on street ventilation, NOx and PM2.5 concentrations across heights in Marylebone Rd street canyon, Central London. Sustain. Cities Soc. 41, 227–241. https://doi.org/10.1016/j.scs.2018.05.030.
Buccolieri, R., Santiago, J.L., Rivas, E., Sanchez, B., 2018b. Review on urban tree modelling in CFD simulations: aerodynamic, deposition and thermal effects. Urban For. Urban Green. 31, 212–220. https://doi.org/10.1016/j.ufug.2018.03.003.
Buccolieri, R., Carlo, O.S., Rivas, E., Santiago, J.L., Salizzoni, P., Siddiqui, M.S., 2022. Obstacles influence on existing urban canyon ventilation and air pollutant concentration: a review of potential measures. Build. Environ. 108905 https://doi.org/10.1016/j.buildenv.2022.108905.
Chatzidimitriou, A., Yannas, S., 2017. Street canyon design and improvement potential for urban open spaces; the influence of canyon aspect ratio and orientation on microclimate and outdoor comfort. Sustain. Cities Soc. 33, 85–101. https://doi.org/10.1016/j.scs.2017.05.019.
Claus, J., Coceal, O., Thomas, T.G., Branford, S., Belcher, S.E., Castro, I.P., 2012. Wind-direction effects on urban-type flows. Bound.-Layer Meteorol. 142, 265–287.
Coceal, O., Goulart, E.V., Branford, S., Thomas, T.G., Belcher, S.E., 2014. Flow structure and near-field dispersion in arrays of building-like obstacles. J. Wind Eng. Ind. Aerodyn. 125, 52–68.
Di Sabatino, S., Buccolieri, R., Olesen, H.R., Ketzel, M., Berkowicz, R., Franke, J., Schatzmann, M., Schlunzen, K., Leitl, B., Britter, R., et al., 2011. COST 732 in practice: the MUST model evaluation exercise. Int. J. Environ. Pollut. 44, 403–418. https://doi.org/10.1504/IJEP.2011.038442.
Di Sabatino, S., Buccolieri, R., Salizzoni, P., 2013. Recent advancements in numerical modelling of flow and dispersion in urban areas: a short review. Int. J. Environ. Pollut. 52, 172–191. https://doi.org/10.1504/IJEP.2013.058454.
EEA, 2020. European Environment Agency. Air Quality in Europe—2020 Report; EEA Report No 09/2020. European Environment Agency, Copenhagen, Denmark. ISSN 1977–8449.
Escobedo, F.J., Nowak, D.J., 2009. Spatial heterogeneity and air pollution removal by an urban forest. Landsc. Urban Plan. 90 (3–4), 102–110.
Fernández-Pampillón, J., Palacios, M., Núñez, L., Pujadas, M., Sanchez, B., Santiago, J.L., Martilli, A., 2021. NOx depolluting performance of photocatalytic materials in an urban area–part I: monitoring ambient impact. Atmos. Environ. 251, 118190 https://doi.org/10.1016/j.atmosenv.2021.118190.
Franke, J., Schlünzen, H., Carissimo, B., 2007. Best Practice Guideline for the CFD Simulation of Flows in the Urban Environment. COST Action 732—Quality Assurance and Improvement of Microscale Meteorological Models; Distributed by University of Hamburg (Germany). Meteorological Institute, Hamburg, Germany. ISBN 3–00–018312-4.
Gallagher, J., Baldauf, R., Fuller, C.H., Kumar, P., Gill, L.W., McNabola, A., 2015. Passive methods for improving air quality in the built environment: a review of porous and solid barriers. Atmos. Environ. 120, 61–70. https://doi.org/10.1016/j.atmosenv.2015.08.075.
Grimmond, C.S.B., Oke, T.R., 1999. Aerodynamic properties of urban areas derived from analysis of surface form. J. Appl. Meteorol. Climatol. 38 (9), 1262–1292.
Gromke, C., Blocken, B., 2015. Influence of avenue-trees on air quality at the urban neighborhood scale. Part II: traffic pollutant concentrations at pedestrian level. Environ. Pollut. 196, 176–184. https://doi.org/10.1016/j.envpol.2014.10.015.
Haaland, C., van Den Bosch, C.K., 2015. Challenges and strategies for urban green-space planning in cities undergoing densification: a review. Urban For. Urban Green. 14 (4), 760–771. https://doi.org/10.1016/j.ufug.2015.07.009.
Holman, C., Harrison, R., Querol, X., 2015. Review of the efficacy of low emission zones to improve urban air quality in European cities. Atmos. Environ. 111, 161–169. https://doi.org/10.1016/j.atmosenv.2015.04.009.
Huang, Y., Lei, C., Liu, C.H., Perez, P., Forehead, H., Kong, S., Zhou, J.L., 2021. A review of strategies for mitigating roadside air pollution in urban street canyons. Environ. Pollut. 280, 116971 https://doi.org/10.1016/j.envpol.2021.116971.
Janhäll, S., 2015. Review on urban vegetation and particle air pollution–deposition and dispersion. Atmos. Environ. 105, 130–137.
Jeanjean, A.P., Buccolieri, R., Eddy, J., Monks, P.S., Leigh, R.J., 2017a. Air quality affected by trees in real street canyons: the case of Marylebone neighbourhood in Central London. Urban For. Urban Green. 2017 (22), 41–53. https://doi.org/10.1016/j.ufug.2017.01.009.
Jeanjean, A.P.R., Gallagher, J., Monks, P.S., Leigh, R.J., 2017b. Ranking current and prospective NO2 pollution mitigation strategies: an environmental and economic modelling investigation in Oxford street. London. Environ. Pollut. 225, 587–597.
Kracht, O., Santiago, J.L., Martin, F., Piersanti, A., Cremona, G., Righini, G., Gerboles, M., 2018. Spatial representativeness of air quality monitoring sites—outcomes of the FAIRMODE/AQUILA Intercomparison exercise. Publications Office of the European Union 2018. https://doi.org/10.2760/60611.
Krayenhoff, E.S., Santiago, J.L., Martilli, A., Christen, A., Oke, T.R., 2015. Parametrization of drag and turbulence for urban neighbourhoods with trees. Boundary-Layer Meteorol. 156 (2), 157–189. https://doi.org/10.1007/s10546-015-0028-6.
Kumar, P., Druckman, A., Gallagher, J., Gatersleben, B., Allison, S., Eisenman, T.S., et al., 2019. The nexus between air pollution, green infrastructure and human health. Environ. Int. 133, 105181.
Li, Z., Ming, T., Shi, T., Zhang, H., Wen, C.Y., Lu, X., Dong, X., Wu, Y., de Richter, R., Li, W., Peng, C., 2021. Review on pollutant dispersion in urban areas-part B: local mitigation strategies, optimization framework, and evaluation theory. Build. Environ. 198, 107890 https://doi.org/10.1016/j.buildenv.2021.107890.
Lien, F.S., Yee, E., 2004. Numerical modelling of the turbulent flow developing within and over a 3-d building array, part I: a high-resolution Reynolds-averaged Navier—stokes approach. Bound.-Layer Meteorol. 112, 427–466.
Livesley, S.J., McPherson, E.G., Calfapietra, C., 2016. The urban forest and ecosystem services: impact on urban water, heat, and pollution cycles at the tree, street and city scale. J. Environ. Qual. 45, 119–124.
Martilli, A., Santiago, J.L., Salamanca, F., 2015. On the representation of urban heterogeneities in mesoscale models. Environ. Fluid Mech. 15, 305–328.
Murena, F., Toscano, D., 2023. Spatial variability of fine particle number concentration in an urban area: the effect of aspect ratio and vehicular traffic. Urban Clim. 52, 101751.
Oke, T.R., 1988. Street design and urban canopy layer climate. Energ. Buildings 11 (1–3), 103–113.
Palacios, M., Núñez, L., Pujadas, M., Fernández-Pampillón, M., Germán, M., Sánchez, B., Santiago, J.L., Martilli, A., Suárez, S., Cabrero, B., 2015. Estimation of NOx deposition velocities for selected comercial photocatalytic products. WIT Trans. Built Environ. 168, 729–740.
Pulvirenti, B., Baldazzi, S., Barbano, F., Brattich, E., Di Sabatino, S., 2020. Numerical simulation of air pollution mitigation by means of photocatalytic coatings in real-world street canyons. Build. Environ. 186, 107348.
Rafael, S., Vicente, B., Rodrigues, V., Miranda, A.I., Borrego, C., Lopes, M., 2018. Impacts of green infrastructures on aerodynamic flow and air quality in Porto's urban area. Atmos. Environ. 190, 317–330. https://doi.org/10.1016/j.atmosenv.2018.07.044.
Richards, P.J., Hoxey, R.P., 1993. Appropriate boundary conditions for computational wind engineering models using the k-ϵ turbulence model. J. Wind Eng. Ind. Aerodyn. 46, 145–153. https://doi.org/10.1016/0167-6105(93)90124-7.
Rivas, E., Santiago, J.L., Lechón, Y., Martín, F., Ariño, A., Pons, J.J., Santamaría, J.M., 2019. CFD modelling of air quality in Pamplona City (Spain): assessment, stations spatial representativeness and health impacts valuation. Sci. Total Environ. 649, 1362–1380. https://doi.org/10.1016/j.scitotenv.2018.08.315.
Roy, S., Byrne, J., Pickering, C., 2012. A systematic quantitative review of urban tree benefits, costs, and assessment methods across cities in different climatic zones. Urban For. Urban Green. 11 (4), 351–363. https://doi.org/10.1016/j.ufug.2012.06.006.
Salmond, J.A., Tadaki, M., Vardoulakis, S., Arbuthnott, K., Coutts, A., Demuzere, M., Dirks, K.N., Heaviside, C., Lim, S., Macintyre, H., et al., 2016. Health and climate related ecosystem services provided by street trees in the urban environment. Environ. Health 15, S36. https://doi.org/10.1186/s12940-016-0103-6.
Sanchez, B., Santiago, J.L., Martilli, A., Palacios, M., Kirchner, F., 2016. CFD modeling of reactive pollutant dispersion in simplified urban configurations with different chemical mechanisms. Atmos. Chem. Phys. 16 (18), 12143–12157. https://doi.org/10.5194/acp-16-12143-2016.
Sanchez, B., Santiago, J.L., Martilli, A., Martin, F., Borge, R., Quaassdorff, C., de la Paz, D., 2017. Modelling NOx concentrations through CFD-RANS in an urban hot-spot using high resolution traffic emissions and meteorology from a mesoscale model. Atmos. Environ. 163, 155–165. https://doi.org/10.1016/j.atmosenv.2017.05.022.
Sanchez, B., Santiago, J.L., Martilli, A., Palacios, M., Núñez, L., Pujadas, M., Fernández-Pampillón, J., 2021. NOx depolluting performance of photocatalytic materials in an urban area-part II: assessment through computational fluid dynamics simulations. Atmos. Environ. 246, 118091 https://doi.org/10.1016/j.atmosenv.2020.118091.
Santamouris, M., Ban-Weiss, G., Osmond, P., Paolini, R., Synnefa, A., Cartalis, C., Muscio, A., Zinzi, M., Morakinyo, T.E., Ng, E., et al., 2018. Progress in urban greenery mitigation science–assessment methodologies advanced technologies and impact on cities. J. Civ. Eng. Manag. 24, 638–671. https://doi.org/10.3846/jcem.2018.6604.
Santiago, J.L., Martilli, A., Martín, F., 2007. CFD simulation of airflow over a regular array of cubes. Part I: three-dimensional simulation of the flow and validation with wind-tunnel measurements. Bound.-Layer Meteorol. 122, 609–634.
Santiago, J.L., Martín, F., Martilli, A., 2013. A computational fluid dynamic modelling approach to assess the representativeness of urban monitoring stations. Sci. Total Environ. 454–455, 61–72. https://doi.org/10.1016/j.scitotenv.2013.02.068.
Santiago, J.L., Borge, R., Martin, F., de la Paz, D., Martilli, A., Lumbreras, J., Sanchez, B., 2017a. Evaluation of a CFD-based approach to estimate pollutant distribution within a real urban canopy by means of passive samplers. Sci. Total Environ. 576, 46–58. https://doi.org/10.1016/j.scitotenv.2016.09.234.
Santiago, J.L., Martilli, A., Martin, F., 2017b. On dry deposition modelling of atmospheric pollutants on vegetation at the microscale: application to the impact of street vegetation on air quality. Boundary-Layer Meteorol. 162 (3), 451–474. https://doi.org/10.1007/s10546-016-0210-5.
Santiago, J.L., Rivas, E., Sanchez, B., Buccolieri, R., Martin, F., 2017c. The impact of planting trees on NOx concentrations: the case of the plaza de la Cruz neighborhood in Pamplona (Spain). Atmosphere 8 (7), 131. https://doi.org/10.3390/atmos8070131.
Santiago, J.L., Buccolieri, R., Rivas, E., Sanchez, B., Martilli, A., Gatto, E., Martín, F., 2019a. On the impact of trees on ventilation in a real street in Pamplona. Spain. Atmosphere 10 (11), 697. https://doi.org/10.3390/atmos10110697.
Santiago, J.L., Buccolieri, R., Rivas, E., Calvete-Sogo, H., Sanchez, B., Martilli, A., Alonso, R., Elustondo, D., Santamaría, J.M., 2019b. Martin, F. CFD modelling of vegetation barrier effects on the reduction of traffic-related pollutant concentration in an avenue of Pamplona, Spain. Sustain. Cities Soc. 48, 101559 https://doi.org/10.1016/j.scs.2019.101559.
Santiago, J.L., Sanchez, B., Quaassdorff, C., de la Paz, D., Martilli, A., Martín, F., Borge, R., Rivas, E., Gómez-Moreno, F.J., Días, E., et al., 2020. Performance evaluation of a multiscale modelling system applied to particulate matter dispersion

in a real traffic hot spot in Madrid (Spain). Atmos. Pollut. Res. 11, 141–155. https://doi.org/10.1016/j.apr.2019.10.001.

Santiago, J.L., Borge, R., Sanchez, B., Quaassdorff, C., De La Paz, D., Martilli, A., Rivas, E., Martín, F., 2021. Estimates of pedestrian exposure to atmospheric pollution using high-resolution modelling in a real traffic hot-spot. Sci. Total Environ. 755, 142475 https://doi.org/10.1016/j.scitotenv.2020.142475.

Santiago, J.L., Sanchez, B., Rivas, E., Vivanco, M.G., Theobald, M.R., Garrido, J.L., Gil, V., Martilli, A., Rodríguez-Sánchez, A., Buccolieri, R., Martín, F., 2022a. High spatial resolution assessment of the effect of the Spanish National air Pollution Control Programme on street-level NO2 concentrations in three neighborhoods of Madrid (Spain) using mesoscale and CFD modelling. Atmosphere 13 (2), 248. https://doi.org/10.3390/atmos13020248.

Santiago, J.L., Rivas, E., Gamarra, A.R., Vivanco, M.G., Buccolieri, R., Martilli, A., Lechón, Y., Martín, F., 2022b. Estimates of population exposure to atmospheric pollution and health-related externalities in a real city: the impact of spatial resolution on the accuracy of results. Sci. Total Environ. 819, 152062 https://doi.org/10.1016/j.scitotenv.2021.152062.

Santiago, J.L., Rivas, E., Buccolieri, R., Martilli, A., Vivanco, M.G., Borge, R., Carlo, O.S., Martín, F., 2022c. Indoor-outdoor pollutant concentration modelling: a comprehensive urban air quality and exposure assessment. Air Qual. Atmos. Health 15, 1583–1608. https://doi.org/10.1007/s11869-022-01204-0.

Santiago, J.L., Rivas, E., Sanchez, B., Buccolieri, R., Esposito, A., Martilli, A., Vivanco, M. G., Martin, F., 2022d. Impact of different combinations of green infrastructure on traffic-related pollutant concentrations in urban areas. Forests 13 (8), 1195. https://doi.org/10.3390/f13081195.

Sanz, C., 2003. A note on k − ε modeling of vegetation canopy air-flows. Bound.-Layer Meteorol. 108, 191–197. https://doi.org/10.1023/A:1023066012766.

Soulhac, L., Salizzoni, P., 2010. Dispersion in a street canyon for a wind direction parallel to the street axis. J. Wind Eng. Ind. Aerodyn. 98 (12), 903–910.

Tomson, M., Kumar, P., Barwise, Y., Perez, P., Forehead, H., French, K., Morawska, L., Watts, J.F., 2021. Green infrastructure for air quality improvement in street canyons. Environ. Int. 2021 (146), 106288 https://doi.org/10.1016/j.envint.2020.106288.

Van den Berg, M., Wendel-Vos, W., van Poppel, M., Kemper, H., van Mechelen, W., Maas, J., 2015. Health benefits of green spaces in the living environment: a systematic review of epidemiological studies. Urban For. Urban Green. 14 (4), 806–816. https://doi.org/10.1016/j.ufug.2015.07.008.

Vardoulakis, S., Solazzo, E., Lumbreras, J., 2011. Intra-urban and street scale variability of BTEX, NO2 and O3 in Birmingham, UK: implications for exposure assessment. Atmos. Environ. 45, 5069–5078. https://doi.org/10.1016/j.atmosenv.2011.06.038.

Vos, P.E., Maiheu, B., Vankerkom, J., Janssen, S., 2013. Improving local air quality in cities: to tree or not to tree? Environ. Pollut. 2013 (183), 113–122. https://doi.org/10.1016/j.envpol.2012.10.021.

Vranckx, S., Vos, P., Maiheu, B., Janssen, S., 2015. Impact of trees on pollutant dispersion in street canyons: a numerical study of the annual average effects in Antwerp. Belgium. Sci. Total Environ. 532, 474–483. https://doi.org/10.1016/j.scitotenv.2015.06.032.

World Health Organization (WHO), 2018. Ambient (outdoor) air quality and health. Fact sheet, Updated May 2018. Available online: https://www.who.int/news-room/fact-sheets/detail/ambient-(outdoor)-air-quality-and-health (accessed on 19 Oct 2022).

Xue, F., Li, X., 2017. The impact of roadside trees on traffic released PM10 in urban street canyon: aerodynamic and deposition effects. Sustain. Cities Soc. 30, 195–204. https://doi.org/10.1016/j.scs.2017.02.001.